$P = 0.139$). The stiffness of the Achilles tendon increased significantly by 28.9 ± 16.4% for WT ($P = 0.002$), but not for PT (21.7 ± 30.5%; $P = 0.109$) (Table 1). There was no significant difference in the relative increase of stiffness between the two protocols ($P = 0.558$).

Table 2 shows the measured variables during the three kinds of jumping tests before and after training. For both protocols, there were no significant differences in the ankle angle at the lowest position in all the jump tasks. The angular velocities at eccentric and concentric phases did not change after training, except for in the concentric phase of SJ for PT ($P = 0.003$). SJ height increased significantly by 29.8 ± 11.8% for PT and 10.9 ± 5.5% for WT (both $P < 0.001$). The PT protocol produced a significant increase in the jump height of CMJ (37.7 ± 23.2%; $P < 0.001$) and DJ (47.5 ± 28.4%; $P < 0.001$), but the WT protocol did not (CMJ: 6.2 ± 9.9%; $P = 0.096$; DJ: 6.5 ± 10.0%; $P = 0.108$). The relative increases in the SJ, CMJ, and DJ heights were significantly greater for PT than for WT (SJ $P < 0.001$; CMJ $P = 0.001$; DJ $P < 0.001$) (Fig. 3). The prestretch augmentation of CMJ and DJ did not change for PT (CMJ $P = 0.161$, DJ $P = 0.075$) and WT (CMJ $P = 0.231$, DJ $P = 0.182$). However, the relative increase in the prestretch augmentation of CMJ was significantly greater for PT than for WT ($P = 0.028$), and that of DJ did not reach statistical significance ($P = 0.058$).

Table 3 shows the mEMG of plantar flexors and TA during jumping tests. The mEMG of plantar flexors during SJ, CMJ, and DJ increased significantly for both PT and WT (all $P < 0.05$). There were no significant differences in the relative increase in the mEMG of plantar flexors between PT and WT. The mEMG of plantar flexors during the other phases (prelanding and eccentric phases) did not change after training using both the protocols. During CMJ and DJ, no changes in the ratio of mEMG of plantar flexors during the eccentric phase to that during the concentric phase were found for both PT and WT (all $P > 0.05$). No significant changes in the mEMG of TA were observed after training.

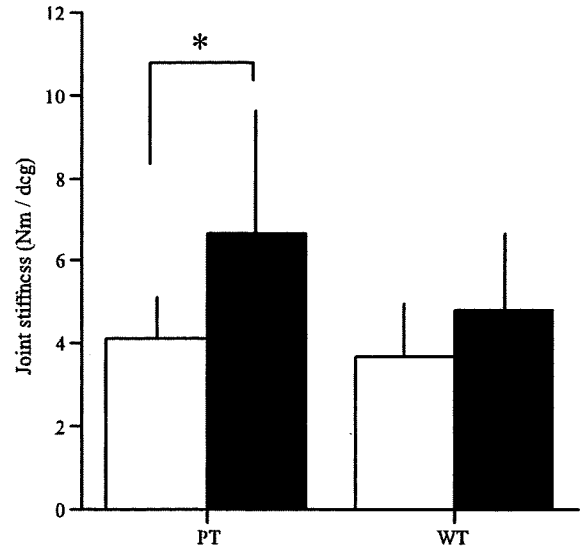

FIGURE 4—The joint stiffness for plyometric (PT) and weight (WT) training protocols before (*open*) and after (*closed*) training. * $P < 0.05$.

The joint stiffness increased significantly from 4.1 ± 1.0 to 6.7 ± 3.0 $N \cdot m \cdot deg^{-1}$ ($P = 0.047$) for PT, but was unchanged for WT ($P = 0.191$) (Fig. 4).

DISCUSSION

The major findings of this study were that 1) the tendon stiffness increased significantly for WT, but not for PT; 2) the joint stiffness increased significantly for PT, but not for WT; 3) the relative increases in the jump heights of SJ, CMJ, and DJ were significantly greater for PT than for WT; and 4) no differences in the changes in the electromyographic

TABLE 3. Electromyographic activities of the plantar flexor and tibial anterior muscles during jumping tests for plyometric and weight training protocols.

	Plyometric Training		Weight Training	
	Before	After	Before	After
Plantar flexor muscles ($mV \cdot s^{-1}$)				
SJ				
CON	0.295 (0.057)	0.386 (0.062)*	0.281 (0.071)	0.355 (0.081)*
CMJ				
ECC	0.113 (0.054)	0.145 (0.036)	0.118 (0.042)	0.128 (0.037)
CON	0.358 (0.045)	0.500 (0.076)*	0.386 (0.058)	0.491 (0.081)*
DJ				
Prelanding	0.087 (0.022)	0.072 (0.038)	0.109 (0.051)	0.071 (0.022)
ECC	0.232 (0.048)	0.275 (0.080)	0.242 (0.095)	0.281 (0.067)
CON	0.292 (0.026)	0.395 (0.045)*	0.308 (0.051)	0.403 (0.070)*
Tibial anterior muscle ($mV \cdot s^{-1}$)				
SJ				
CON	0.058 (0.013)	0.062 (0.015)	0.063 (0.020)	0.067 (0.021)
CMJ				
ECC	0.035 (0.022)	0.054 (0.021)	0.041 (0.017)	0.059 (0.040)
CON	0.108 (0.036)	0.103 (0.030)	0.111 (0.024)	0.099 (0.018)
DJ				
Prelanding	0.061 (0.033)	0.074 (0.040)	0.078 (0.041)	0.055 (0.027)
ECC	0.172 (0.047)	0.129 (0.038)	0.178 (0.081)	0.113 (0.033)
CON	0.135 (0.036)	0.116 (0.046)	0.135 (0.046)	0.105 (0.015)

Mean (SD).
* Significantly different from before training.

activities of measured muscles during jumping were found between PT and WT.

Previous findings obtained from animal experiments demonstrated that the mechanical and morphological properties of tendons were variable through physical training (2,25,28,30,32,34). Most of these previous studies used endurance exercises as the training protocol, and revealed increases in the ultimate failure load and stiffness of tendons. In contrast, Simonsen et al. (28) report that strength training produced no significant changes in the ultimate tensile strength of the rat Achilles tendon. Further, only a few attempts have so far been made at investigating the influences of plyometric training on tendons (25,30). According to the limited information available, jumping or sprint training protocols produced no significant changes in tendon properties (25,30). With regard to the effect of plyometric training on human tendons, cross-sectional information is available from previous research (11,15). We have reported that the tendon properties of knee extensors were more compliant in sprinters compared with untrained subjects (15). Recently, we have shown that that the tendon properties of knee extensors did not change after repeated drop jump exercises temporarily (14). Furthermore, our previous study has demonstrated that the tendon stiffness of knee extensors increased after 12 wk of isometric training (12). In addition to this, other types of isometric training (short duration of muscle contraction), characterized as *ballistic* or *explosive*, did not increase the stiffness of tendon structures (12). Considering these previous findings using animals and humans (12,14,15,25,30), an exercise protocol that required high force production for a short duration (i.e., ballistic contraction) could not change the tendon properties.

Recent studies have demonstrated that the stiffness of human tendons increased after resistance training using a heavy load (12,18,27). The present results for the WT protocol agreed with these previous findings. However, the training protocol did not induce a significant hypertrophic change in the tendons. A possible explanation would be that the resistance training induced changes in the internal structures of tendons. Namely, the variability of the mechanical quality of tendon structures originates from differences in the cross-link pattern or structure of the collagen fibers (5). On the other hand, according to our recent observations concerning changes in tendon stiffness after training, the increase of tendon stiffness after isometric training (e.g., 58% (12)) tended to be greater than that after isotonic training (e.g., 30% (17); 29% (present study)). Hence, it might be assumed that there was a difference in the effects of the contraction mode on the tendon properties between isometric and dynamic contractions. Unfortunately, the mechanisms which resulted in the increase of tendon stiffness after isometric and isotonic training protocols are unknown. These areas are presently under investigation in our laboratory.

Some previous researchers have suggested that enhanced jumping performance after plyometric training was attributed to neural adaptations, that is, the patterns of motor unit recruitment and muscle activities of agonists and antagonists (3,4,6,21,33). For example, Chimera et al. (3) report that the adductor muscle preactivation and adductor and abductor coactivation both increased after plyometric training. In the present study, however, the relative increases in jump heights were greater for PT than for WT (Fig. 3). If these differences in jump performances were caused by neural adaptations, the changes in the EMG activities during jumping would be different between PT and WT protocols. For all jumping tasks, however, no differences in the increase in mEMG during the concentric phase were found between PT and WT (Table 3). In addition, the mEMG of plantar flexors and TA during the other phases (prelanding and eccentric phases) did not change after training (Table 3). Kyrolainen et al. (20) also have demonstrated that the muscle activity patterns did not change after 15 wk of plyometric training. They state that the increases in the jump height after plyometric training cannot be explained by changes in the muscle activity patterns and/or increased neural input to the muscles. Therefore, these results suggested that the differences in jump heights between PT and WT were not caused by the muscle activation strategies.

In the present study, the maximal tendon elongation and stored elastic energy increased significantly in the PT protocol (Table 1). Thus, the increases in the CMJ and DJ heights for PT would be related to the unchanged tendon stiffness. Hence, it might be assumed that, compared with the WT protocol, the tendon properties would change to be suitable for stretch-shortening cycle exercises after plyometric training. For WT, on the contrary, the jump heights of CMJ and DJ did not change after training. This result could also be explained by an offset of the positive (increase in muscle function) and negative (increase in tendon stiffness) effects on performance during stretch-shortening cycle exercises. This point was already confirmed by our recent study (18). Namely, isometric squat training increased the tendon stiffness of knee extensors and decreased prestretch augmentation during vertical jumping. However, the performance during stretch-shortening cycle exercises cannot be explained by only one factor (tendon property), since this is a complex issue. These discussions require additional data for clarification.

Another finding of this study was that the joint stiffness increased significantly for PT, but not for WT (Fig. 4). This result agrees with the previous findings (29,31). Komi (10) suggests that a higher stiffness level of lower-limb muscles during stretch-shortening cycle exercises facilitated greater amounts of stored and reused elastic energy. In fact, Heise and Martin (7) show a positive correlation between leg stiffness and running economy, concluding that economical runners possessed a running style that was stiffer during ground contact. Furthermore,

Toumi et al. (31) suggest that the high joint stiffness during the eccentric phase might be accomplished by a proper preprogrammed motor command. At the beginning of the study, therefore, it was expected that the increase in joint stiffness would be the result of neural adaptations after training. In the present results, however, there were no significant differences in the changes induced by the two protocols in muscle activities during jumping. Accordingly, we may say that the increase in joint stiffness after plyometric training was caused by changes in the mechanical properties of muscle–tendon complex, and not by neural adaptations. Malisoux et al. (23) report that the passive tension of a single muscle fiber increased after 8 wk of plyometric training. They also stated that plyometric training was effective in improving the cross-bridge mechanics of single fibers. Taking the present findings into account along with these previous findings, it is likely that the increase in joint stiffness after plyometric training is related to the changes in the properties of muscle (active cross-bridge), because of unchanged tendon stiffness.

Recent studies showed that running economy and performance improved after plyometric training (26,29). Spurrs et al. (29) report that plyometric training improved running economy and distance running performance, and thus increased the musculotendinous stiffness of the ankle joint using the oscillation technique. They postulated that the increase in the musculotendinous stiffness of the ankle joint resulted in improved running economy and performance. Taking these previous findings into account, together with our results on the PT protocol, we speculate that tendon stiffness remained unchanged and that joint stiffness increased after plyometric training. These changes in the mechanical properties of muscle–tendon complex would lead to the improved running economy and distance running performance.

In conclusion, tendon stiffness increased by weight training; conversely, joint stiffness increased by plyometric training. Furthermore, jump performance improved by plyometric training, although no differences in the pattern of muscle activities during jumping were found between before and after training. These results indicate that the jump performance gains after plyometric training are attributed to changes in the mechanical properties of muscle–tendon complex, rather than muscle activation strategies.

REFERENCES

1. Bojsen-Moller, J., S. P. Magnusson, L. R. Rasmussen, M. Kjaer, and P. Aagaard. Muscle performance during maximal isometric and dynamic contractions is influenced by the stiffness of the tendinous structures. *J. Appl. Physiol.* 99:986–994, 2005.
2. Buchanan, C. I., and R. L. Marsh. Effects of long-term exercise on the biomechanical properties of the Achilles tendon of guinea fowl. *J. Appl. Physiol.* 90:164–171, 2001.
3. Chimera, N. J., K. A. Swanikt, C. Buz Swanikt, and S. J. Straub. Effects of plyometric training on muscle-activation strategies and performance in female athletes. *J. Athl. Train.* 39:24–31, 2004.
4. Cutsem, M. V., J. Duchateau, and K. Hainaut. Changes in single motor unit behaviour contribute to the increase in contraction speed after dynamic training in humans. *J. Physiol.* 513:295–305, 1998.
5. Danielsen, C. C., and T. T. Andereassen. Mechanical properties of rat tail tendon in relation to proximal-distal sampling position and age. *J. Biomech.* 21:207–212, 1988.
6. Hakkinen, K., A. Pakarinen, H. Kyrolainen, S. Cheng, D. H. Kim, and P. V. Komi. Neuromuscular adaptations and serum hormones in females during prolonged power training. *Int. J. Sports Med.* 11:91–98, 1990.
7. Heise, G. D., and P. E. Martin. "Leg spring" characteristics and the aerobic demand of running. *Med. Sci. Sports Exerc.* 30: 750–754, 1998.
8. Kaneko, M., T. Fuchimoto, H. Toji, and K. Suei. Training effect of different loads on the force-velocity relationship and mechanical power output in human muscle. *Scand. J. Sports Sci.* 5:50–55, 1983.
9. Kawakami, Y., T. Muraoka, S. Ito, H. Kanehisa, and T. Fukunaga. In vivo muscle fibre behaviour during counter-movement exercise in humans reveals a significant role for tendon elasticity. *J. Physiol.* 540:635–646, 2002.
10. Komi, P. V. *Stretch-Shortening Cycle.* London, UK: Blackwell Science, 1992.
11. Kongsgaard, M., P. Aagaard, M. Kjaer, and S. P. Magnusson. Structural Achilles tendon properties in athletes subjected to different exercise modes and in Achilles tendon rupture patients. *J. Appl. Physiol.* 99:1965–1971, 2005.
12. Kubo, K., H. Kanehisa, and T. Fukunaga. Effects of different duration isometric contractions on tendon elasticity in human quadriceps muscles. *J. Physiol.* 536:649–655, 2001.
13. Kubo, K., H. Kanehisa, and T. Fukunaga. Effects of resistance and stretching training programs on the viscoelastic properties of tendon structures in vivo. *J. Physiol.* 538:219–226, 2002.
14. Kubo, K., H. Kanehisa, and T. Fukunaga. Influences of repetitive drop-jump and isometric leg press exercises on the tendon properties in knee extensors. *J. Strength Cond. Res.* 19:864–870, 2005.
15. Kubo, K., H. Kanehisa, Y. Kawakami, and T. Fukunaga. Elasticity of tendon structures of lower limbs in sprinters. *Acta Physiol. Scand.* 168:327–335, 2000.
16. Kubo, K., Y. Kawakami, and T. Fukunaga. Influence of elastic properties of tendon structures on jump performance in humans. *J. Appl. Physiol.* 87:2090–2096, 1999.
17. Kubo, K., T. Komuro, N. Ishiguro, et al. Effects of low load resistance training with vascular occlusion on the mechanical properties of muscle and tendon. *J. Appl. Biomech.* 22:112–119, 2006a.
18. Kubo, K., H. Yata, H. Kanehisa, and T. Fukunaga. Effects of isometric squat training on the tendon stiffness and jump performance. *Eur. J. Appl. Physiol.* 96:305–314, 2006.
19. Kuitunen, S., J. Avela, H. Kyrolainen, C. Nicol, and P. V. Komi. Acute and prolonged reduction in joint stiffness in humans after exhausting stretch-shortening cycle exercise. *Eur. J. Appl. Physiol.* 88:107–116, 2002.
20. Kyrolainen, H., J. Avela, J. M. McBride, et al. Effects of power training on mechanical efficiency in jumping. *Eur. J. Appl. Physiol.* 91:155–159, 2004.
21. Kyrolainen, H., P. V. Komi, and D. H. Kim. Effects of power training on neuromuscular performance and mechanical efficiency. *Scand. J. Med. Sci. Sports* 1:78–87, 1991.

22. MAGNUSSON, S. P., P. AAGAARD, S. ROSAGER, P. D. POULSEN, and M. KJAER. Load-displacement properties of the human triceps surae aponeurosis in vivo. *J. Physiol.* 531:277–288, 2001.
23. MALISOUX, L., M. FRANCAUX, H. NIELENS, and D. THEISEN. Stertch-shortening cycle exercises: an effective training paradigm to enhance power output of human single muscle fibers. *J. Appl. Physiol.* 100:771–779, 2006.
24. MCDONAGH, M. J. N., and C. T. M. DAVIES. Adaptive response of mammalian skeletal muscle to exercise with high loads. *Eur. J. Appl. Physiol.* 52:139–155, 1984.
25. NAKAGAWA, Y., T. SATOH, Y. FUKUDA, and K. HIROTA. Effect of aerobic and anaerobic training on collagen fibers of tendons in rats. *J. Phys. Fitness Sports Med.* 37:100–108, 1988.
26. PAAVOLAINE, L., K. HAKKINEN, I. HAKKINEN, A. NUMMELA, and H. RUSKO. Explosive-strength training improves 5-km running time by improving running economy and muscle power. *J. Appl. Physiol.* 86:1527–1533, 1999.
27. REEVES, N. D., C. N. MAGANARIS, and M. V. NARICI. Effect of strength training on human patella tendon mechanical properties of older individuals. *J. Physiol.* 548:971–981, 2003.
28. SIMONSEN, R. B., H. KLITGAARD, and F. BOJSEN-MOLLER. The influence of strength training, swim training and aging on the Achilles tendon and m. soleus of the rat. *J. Sports Sci.* 13: 291–295, 1995.
29. SPURRS, R. W., A. J. MURPHY, and M. L. WATSFORD. The effect of plyometric training on distance running performance. *Eur. J. Appl. Physiol.* 89:1–7, 2003.
30. TIPTON, C. M., R. D. MATHES, J. A. MAYNARD, and R. A. CAREY. The influence of physical activity on ligaments and tendons. *Med. Sci. Sports* 7:165–175, 1975.
31. TOUMI, H., T. M. BEST, A. MARTIN, and G. POUMARAT. Muscle plasticity after weight and combined (weight + jump) training. *Med. Sci. Sports Exerc.* 36:1580–1588, 2004.
32. VILARTA, R., and C. VIDAL BDE. Anisotropic and biomechanical properties of tendons modified by exercise and denervation: aggregation and macromolecular order in collagen bundles. *Matrix* 9:55–61, 1989.
33. WILK, K. E., M. L. VOIGHT, M. A. KEIRNS, V. GAMBETTA, J. R. ANDREWS, and C. J. DILLMAN. Stretch-shortening drills for the upper extremities: theory and clinical application. *J. Orthop. Sports Phys. Ther.* 17:225–239, 1993.
34. WOO, S. L., M. A. GOMEZ, D. AMIEL, M. A. RITTER, R. H. GELBERMAN, and W. H. AKESON. The effects of exercise on the biomechanical and biochemical properties of swine digital flexor tendons. *J. Biomech. Eng.* 103:51–56, 1981.

J Appl Physiol 103: 1688–1695, 2007.
First published August 30, 2007; doi:10.1152/japplphysiol.00255.2007.

Applicability of a segmental bioelectrical impedance analysis for predicting the whole body skeletal muscle volume

Noriko I. Tanaka,[1] Masae Miyatani,[2] Yoshihisa Masuo,[3] Tetsuo Fukunaga,[3] and Hiroaki Kanehisa[4]

[1]*Department of Sport System, Kokushikan University, Tokyo, Japan;* [2]*Rehabilitation Engineering Laboratory, Lyndhurst Centre Toronto Rehabilitation Institute, Toronto, Ontario, Canada;* [3]*Department of Sport Sciences, School of Human Sciences, Waseda University, Saitama, Japan; and* [4]*Department of Life Sciences (Sports Sciences), University of Tokyo, Tokyo, Japan*

Submitted 5 March 2007; accepted in final form 23 August 2007

Tanaka NI, Miyatani M, Masuo Y, Fukunaga T, Kanehisa H. Applicability of a segmental bioelectrical impedance analysis for predicting the whole body skeletal muscle volume. *J Appl Physiol* 103: 1688–1695, 2007. First published August 30, 2007; doi:10.1152/japplphysiol.00255.2007.—This study aimed to test the hypothesis that a segmental bioelectrical impedance (BI) analysis can predict whole body skeletal muscle (SM) volume more accurately than a whole body BI analysis. Thirty males (19–34 yr) participated in this study. They were divided into validation (n = 20) and cross-validation groups (n = 10). The BI values were obtained using two methods: whole body BI analysis, which determines impedance between the wrist and ankle; and segmental BI analysis, which determines the impedance of every body segment in both sides of the upper arm, lower arm, upper leg and lower leg, and five parts of the trunk. Using a magnetic resonance imaging method, whole body SM volume was determined as a reference (SMV_{MRI}). Simple and multiple regression analyses were applied to $(length)^2/Z$ (BI index) for the whole body and for every body segment, respectively, to develop the prediction equations of SMV_{MRI}. In the validation group, there were no significant differences between the measured and estimated SMV and no systematic errors in either BI analysis. In the cross-validation group, the whole body BI analysis produced systematic errors and resulted in the overestimation of SMV_{MRI}, but the segmental BI analysis was cross-validated. In the pooled data, the segmental BI analysis produced a prediction equation, which involves the BI indexes of the trunk and upper thigh as independent variables, with a SE of estimation of 1,693.8 cm^3 (6.1%). Thus the findings obtained here indicated that the segmental BI analysis is superior to the whole body BI analysis for estimating SMV_{MRI}.

human body composition; magnetic resonance imaging; muscle distribution; validation; cross-validation

THE QUALITATIVE ASSESSMENT of human skeletal muscle (SM) mass helps us to evaluate physical resources in relation to physical performance in daily life and/or sporting activities (16). There is increasing interest in the use of bioelectrical impedance (BI) analysis to estimate SM mass because it is safe, noninvasive, convenient, easy, and inexpensive (3). However, little information on the validity of BI analyses for estimating whole body SM mass is available. To our knowledge, only Janssen et al. (14) have tried to estimate whole body SM mass using a BI analysis in which the BI value between the right wrist and right leg was obtained. In their results, however, the developed prediction equation produced a systematic error and overestimated whole body SM mass. The BI analysis taken in the prior study has been referred to as "whole body BI analysis" (3, 5, 9, 14, 19), although the electric current in this technique has been shown to be passed thorough the whole trunk and one side of the extremities (9). When a whole body BI analysis is used to estimate whole body SM mass, the human body is assumed to be a cylindrical and isotrophic conductor with a uniform cross-sectional area (CSA). However, the whole body BI value depends strongly on the variation in the CSA of the lower arm and lower leg (4, 8, 9). Moreover, it has been reported that the change in the trunk SM volume hardly affects the whole body BI value (9). Considering these points, it is hypothesized that the BI value obtained by the whole body BI analysis may be mostly affected by SM mass in the distal parts of limbs, and so this would be a reason for the systematic error in the estimates of whole body SM mass with the whole body BI analysis (14). However, no study has examined this assumption.

As another technique of the BI analysis, Organ et al. (19) developed various combinations of electrodes to determine the BI value of every body segment, i.e., a segmental BI analysis. A prior study (12) that used a subject sample with a large variation in muscularity found that, compared with the whole body BI analysis, a segmental BI analysis that measured BI values from proximal segments of the human body (i.e., upper arm, upper leg, and whole trunk) could predict lean body mass without influence from differences in the lean tissues between the proximal and distal parts (lower arms and lower legs) of the body segments. The segmental BI analysis can be used to estimate the limb SM volume through comparison with that determined by magnetic resonance imaging (MRI) (2, 17, 18). In addition, Ishiguro et al. (13) indicated that the segmental BI analysis could be applicable to the estimation of trunk SM volume. Taking these findings into account, it may be assumed that the prediction equation developed from a segmental BI analysis, which involves the BI indexes of the upper arm, upper leg, and trunk as the independent variables, can predict whole body SM mass with a higher degree of accuracy compared with that developed from a whole body BI analysis. The present study aimed to test this hypothesis. To this end, we measured BI values using the whole body and segmental BI analyses in young adult men, including athletes, who formed a heterogeneous sample with respect to body physique and muscular development. Some data on the physical charac-

Address for reprint requests and other correspondence: N. I. Tanaka, Dept. of Sport System, Kokushikan Univ., 7-3-1 Nagayama, Tama-shi, Tokyo 206-8515, Japan.

The costs of publication of this article were defrayed in part by the payment of page charges. The article must therefore be hereby marked "*advertisement*" in accordance with 18 U.S.C. Section 1734 solely to indicate this fact.

teristics of subjects and the trunk SM volume have been reported elsewhere (13).

METHODS

Subjects. Thirty healthy Asian males (19–34 yr) voluntarily participated in this study. Fourteen of the subjects were athletes (8 American football players, 3 power lifters, 1 weight lifter, 1 triathlete, and 1 baseball player) who had participated in competitive meets in their own events at the college level within a year preceding the measurements. The remainder were either sedentary or mildly active, but none was currently involved in any type of exercise program (≥30 min/day, ≥2 days/wk). To confirm the cross-validity of the predicting equation, the subjects were randomly separated into a validation group (n = 20) and a cross-validation group (n = 10), in which the percentage of the number of athletes to the total number of subjects was almost the same, i.e., 10 athletes in the validation group and 4 athletes in the cross-validation group. Physical characteristics of each subject group are listed in Table 1. Data for the athletes were collected during preseason training. Therefore, none of the athletes were dehydrated to control their body mass for competition. All measurements for the athletes were performed more than 40 h after completion of a training session. This study was approved by the ethics committee of the Department of Life Sciences, Graduate School of Arts and Sciences, University of Tokyo, and was consistent with their requirements for human experimentation. The subjects were fully informed about the procedures and the purpose of this study. Written informed consent was obtained from all participants.

Anthropometric measurements. Body height was measured to the nearest 0.1 cm on a standard physician's scale. The body mass was measured to the nearest 0.1 kg on a calibrated electric scale. The lengths of the limb on the right side of the body were measured to the nearest 0.5 cm with a flexible metal tape (Flat rule, KDS). In this study, the length of every body segment was defined as the distance between the electrodes placed to determine the segmental BI values in accordance with the prior study (11): upper arm, distance between the acromion process and the lateral epicondyle of the humerus ($L_{\text{upper arm}}$); lower arm, distance between the head of the radius and the processus styloideus ($L_{\text{lower arm}}$); upper leg, distance between the greater trochanter of the femur and articular cleft between the femoral and tibial condyles ($L_{\text{upper leg}}$); lower leg, distance between the malleolus lateralis and the articular cleft between the femoral and tibial condyles ($L_{\text{lower leg}}$). The distance between the acromion process of the right shoulder and the greater trochanter of the right femur was measured from MRI images and defined as the trunk length (L_{TR}).

Table 1. *Descriptive data on physical characteristics and MRI-measured tissue volume of subjects*

Variables	Validation Group (n = 20)		Cross-Validation Group (n = 10)		Total (n = 30)	
	Mean	SD	Mean	SD	Mean	SD
Age, yr	24.5	2.8	24.2	4.1	24.4	3.2
Height, cm	175.4	5.0	174.2	5.9	175.0	5.2
Body mass, kg	77.8*	10.7	73.0	7.3	76.2	9.8
BMI, kg/m^2	25.3	3.3	24.1	2.4	24.9	3.1
Segment length, cm						
Upper arm	33.2	1.2	32.9	1.7	33.1	1.4
Lower arm	24.4	1.0	24.2	1.2	24.3	1.0
Upper leg	40.9	1.4	40.9	1.9	40.9	1.6
Lower leg	40.4	1.7	40.2	2.0	40.3	1.8
Trunk	61.0	2.8	58.4	3.0	60.1	3.1

n = no. of men/group. BMI, body mass index. *Mean value is significantly different from that for the cross-validation group at $P < 0.05$.

MRI measurements. With the use of MRI scans taken with a body coil (Airis, Hitachi Medco), a series of transverse images from the acromion process to the malleolus lateralis was obtained. The image condition was T1 weighted, spin-echo, multislice sequences with a slice thickness of 10 mm and a slice interval of 20 mm, with a repetition time of 200 ms and an echo time of 20 ms. Each subject lay supine in the body coil with his arms and legs extended and relaxed. We defined the whole body SM volume as the sum of trunk and limb SM volumes (4). The trunk SM was separated from limbs by using slices between specific landmarks, the acromion process of the shoulder and the greater trochanter of the femur (4). Therefore, some SM located in the shoulder and/or gluteus (i.e, triangular and/or gluteal muscle) were partially analyzed as the trunk SMs. From each cross-sectional image, outlines of tissues (SM, subcutaneous fat, bone, visceral, and others) were traced and digitized by personal computer (Power Macintosh G4, Apple) to calculate the anatomic CSA of every tissue. Adipose and tendinous tissues, which were imaged in different tones from the muscle tissue, were excluded when digitizing. We removed as much of intramuscular adipose tissue areas as possible from the SM and categorized those as "others." By summing the anatomic SM CSA and then multiplying the sum by the interval of 20 mm, whole body SM volume was determined and referred to as SMV_{MRI}.

The test-retest variability of SMV_{MRI} was assessed with 10 men (22–26 yr) on two separate days. The intraclass correlation coefficient for the test-retest measurements was 0.990 and the coefficient of variation (CV) was 1.8. There was no significant difference between the mean values of the two tests. Again, the intraobserver reproducibility was assessed by analyzing the MRI images of 5 men (22–26 yr) two times. The intraclass correlation coefficient and the CV of SMV_{MRI} values from the two trials were 0.951 and 2.9, respectively. There was no significant difference between the mean values of the two trials.

BI measurements. A BI acquisition system (Muscle α, Art Haven 9) and the disposable electrodes (Red Dot 2330, 3M) were used to determine the BI values of the whole body and each body segment. This system applies a constant current of 500 μA and frequency of 50 kHz through the body. The measured BI value was referred to as Z. The BI measurements were performed on different days from the MRI measurements with an interval of 1 or 2 days. The subjects refrained from vigorous exercise and alcohol intake for 24 h, and from taking a meal for 4 h, preceding the experiments. All BI measurements were carried out in the supine position, with the arms relaxed at the side but not touching the body and the legs separated at least 25.0 cm at the ankles so that there was no contact between the upper legs. The subjects were instructed to keep breathing quietly because the respiratory cycle affected the trunk Z (7). During the measurements, room temperature was kept at 23°C (8).

The electrode placement is shown in Fig. 1. The source electrodes were placed at the dorsal surface of the third metacarpal bone of the right hand and the dorsal surface of the third metatarsal bone of the right foot for the whole body BI analysis, and the dorsal surface of the third metacarpal bone of both hands and the dorsal surface of the third metatarsal bone of both feet for the segmental BI analysis. The detector electrode placement was as follows: for the measurement of whole body Z ($Z_{\text{whole body}}$), at the dorsal surface of the right wrist at the level of the hand of radial and ulnar bones and anterior surface of the right ankle between the protruding portions of the tibial and fibular bones; for the upper arm Z ($Z_{\text{upper arm}}$), at the dorsal surface of both elbows between the lateral epicondyles of the humerus and the head of the radius and the acromion process of both shoulders; for the lower arm Z ($Z_{\text{lower arm}}$), at the dorsal surfaces of both wrists at the level of the head of radial and ulnar bones and the dorsal surface of both elbows between the lateral epicondyles of the humerus and the head of the radius; for the upper leg Z ($Z_{\text{upper leg}}$), at the articular cleft between the femoral and tibial condyles of both legs and the greater trochanter of both femurs; and for the lower leg Z ($Z_{\text{lower leg}}$), at the

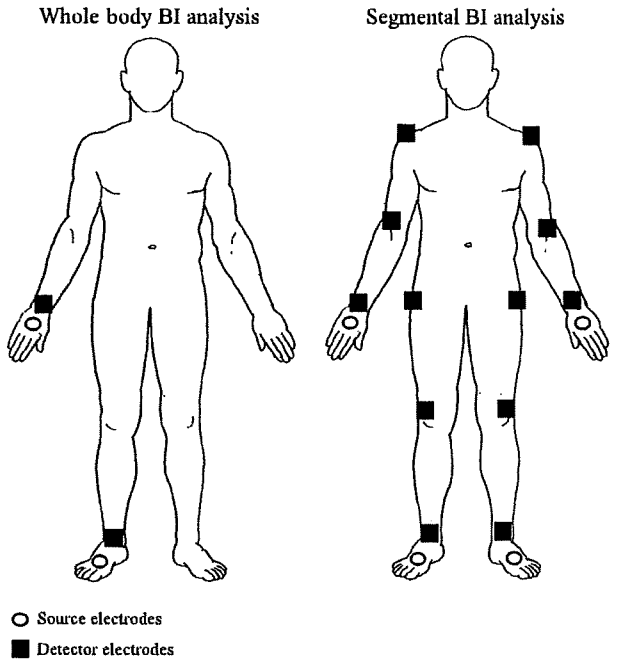

Fig. 1. Schematic representations of the positions of electrodes for bioelectrical impedance (BI) analyses.

anterior surface of both ankles between the protruding portions of the tibial and fibular bones and the articular cleft between the femoral and tibial condyles of both legs. For the trunk BI measurement, the detector electrodes were placed at the acromion process of both shoulders and the greater trochanter of both femurs. This combination of electrodes can measure Z from five regions: both sides of the upper trunk (Z_{TRur} and Z_{TRul}), the middle trunk (Z_{TRm}), and both sides of the lower trunk (Z_{TRlr} and Z_{TRll}) (13). The whole trunk Z ($Z_{TRwhole}$) can be calculated with the following equation using each BI measurement

$$Z_{TRwhole} = (Z_{TRur} \times Z_{TRul})/(Z_{TRur} + Z_{TRul}) + Z_{TRm} + (Z_{TRlr} \times Z_{TRll})/(Z_{TRlr} + Z_{TRll})$$

The BI indexes of the whole body and each body segment were calculated as follows

$$\text{BI index of whole body} = (\text{height})^2/Z_{\text{whole body}}$$

$$\text{BI index of upper arm} = (L_{\text{upper arm}})^2/[Z_{\text{upper arm}}(\text{right side}) + Z_{\text{upper arm}}(\text{left side})]$$

$$\text{BI index of lower arm} = (L_{\text{lower arm}})^2/[Z_{\text{lower arm}}(\text{right side}) + Z_{\text{lower arm}}(\text{left side})]$$

$$\text{BI index of upper leg} = (L_{\text{upper leg}})^2/[Z_{\text{upper leg}}(\text{right side}) + Z_{\text{upper leg}}(\text{left side})]$$

$$\text{BI index of lower leg} = (L_{\text{lower leg}})^2/[Z_{\text{lower leg}}(\text{right side}) + Z_{\text{lower leg}}(\text{left side})]$$

$$\text{BI index of trunk} = (L_{TR})^2/Z_{TRwhole}$$

The test-retest variability of the Z values and BI indexes was assessed with 23 men (19–30 yr) on two separate days. The intraclass correlation coefficients and the %CV were 0.839–0.978 and 1.6–2.9% for each Z value. There were no significant differences in each Z value between the two tests.

Data analysis. Descriptive values were presented as means and standard deviations (SDs). In the validation group, first, the equations were developed for predicting the measured SMV_{MRI} with the use of the BI indexes as independent variables, determined in each of the whole body and the segmental BI analyses. For the whole body BI analysis, a simple regression analysis was applied to develop a prediction equation for SMV_{MRI} with $(\text{height})^2/Z_{\text{whole body}}$ as an independent variable. For the segmental BI analysis, the multiple regression analysis was used to develop the prediction equation for SMV_{MRI} using the BI indexes in the upper arm, upper leg, and trunk as the independent variables. The estimated whole body SM volume was referred to as SMV_{BI}; $SMV_{\text{whole body BI}}$ refers to the whole body BI analysis and $SMV_{\text{segmental BI}}$ for the segmental BI analysis. For every independent variable selected, the product of the standard regression coefficient in the multiple regression equation and the simple correlation coefficient in the relationship with SMV_{MRI}, expressed as a percentage, was calculated as an index presenting its relative contribution to the estimation of SMV_{MRI}. Second, it was confirmed that the regression slope and intercept for the relationship between the SMV_{MRI} and SMV_{BI} values did not significantly differ from 1 and 0, respectively. Again, the significance of the difference between SMV_{MRI} and SMV_{BI} was confirmed using Student's paired t-test. The SE of the estimate (SEE) was calculated to evaluate the accuracy of SMV_{BI}. The SEE was expressed as an absolute value and relative to the mean of SMV_{MRI}. Third, the residual ($SMV_{MRI} - SMV_{BI}$) was plotted against the mean SMV for the two methods to examine for systematic error, as described by Bland and Altman (6). When the three conditions mentioned above were satisfied, SMV_{BI} was calculated for the individuals of the cross-validation group using the equation derived from the validation group. The cross-validity of the prediction equation was examined by the same three steps as used for the validation group. If either or both of the prediction equations were cross-validated, the data from the two groups were pooled to generate the final equation, and the standard regression coefficient of each independent variable was calculated. With regard to the final equation, too, the accuracy was confirmed by the same three steps as mentioned above. A simple linear regression analysis was used to calculate the correlation coefficient (r). The probability level for statistical significance was set at $P < 0.05$.

RESULTS

Baseline characteristics of the validation and cross-validation groups. Table 1 shows the descriptive data on the physical characteristics in the validation and cross-validation groups. There were no significant differences between the two groups in any variables except for body mass.

Figure 2 shows the distribution of the measured SM CSA in every body segment, plotted at every 10% of the segment length. The largest SM CSA was observed at 10% L_{TR}, and the second one at 90% L_{TR}.

The SM volumes of the whole body and every body segment determined by MRI did not differ between the validation and cross-validation groups (Table 2). Moreover, there were no significant differences between the groups in the measured Zs and BI indexes (Table 3).

Prediction equation derived from the validation group. The whole body BI index was significantly correlated to the SMV_{MRI} ($r = 0.883$, $P < 0.05$) in the validation group. This relationship produced an equation, $SMV_{\text{whole body BI}} = 422.2 \times [(\text{height})^2/Z_{\text{whole body}}] - 1{,}201.4$, with R^2 and SEE values of 0.779 and 2,180.6 cm^3 (7.7%), respectively.

In the segmental BI analysis, the BI indexes of the upper leg and trunk were selected as significant contributors to predict SMV_{MRI} (Fig. 3) and produced an equation, $SMV_{\text{segmental BI}} =$

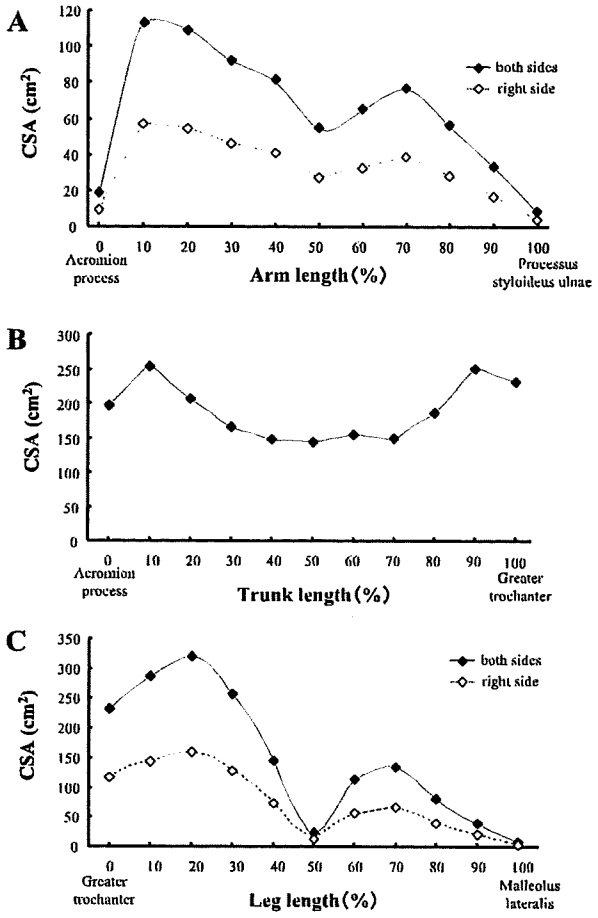

Fig. 2. Distribution of skeletal muscle cross-sectional area (CSA) in the whole body. ◆, Sum of the CSAs in both sides of the body; ◇, CSAs in right side of the body.

$129.1 \times [(L_{TR})^2/Z_{TRwhole} + 1{,}241.3 \times (L_{upper\ leg})^2/Z_{upper\ leg}] - 6{,}844.1$, with R^2 and SEE values of 0.852 and 1,866.0 cm^3 (6.6%), respectively. The relative contribution of each of the two BI indexes to the prediction of SMV_{MRI} was 51.9% for the upper leg and 33.7% for the trunk. Even if the BI index of the upper arm was entered as the predictive variable, R^2 (0.856) and SEE (1,844.8 cm^3, 6.5%) were similar as those in the equation using the BI indexes of the upper leg and trunk.

The regression analyses indicated that the slopes and intercepts of the regression equations for the relationship between SMV_{MRI} and SMV_{BI} were not significantly different from 1 and 0, respectively, in the whole body and segmental BI analyses (Fig. 4, *A* and *B*). In addition, there were no significant differences between the measured and estimated SMVs in the two BI analyses. Again, no significant systematic errors were found in the Bland-Altman plots for the whole body [r = 0.257, nonsignificant (NS)] and segmental (r = 0.204, NS) BI analyses (Fig. 4, *C* and *D*).

Cross-validation of the prediction equation. The prediction equation derived from the validation group was used to estimate SMV_{MRI} in the cross-validation group. The slopes and intercepts of the regression equations for the relationships between SMV_{MRI} and either $SMV_{whole\ body\ BI}$ or $SMV_{segmental\ BI}$ were not significantly different from 1 and 0, respectively (Fig. 5, *A* and *B*). However, the Bland-Altman plot for the whole body BI analysis indicated that $SMV_{whole\ body\ BI}$ tended to be influenced by the magnitude of SMV_{MRI} (r = −0.635, $P < 0.05$) (Fig. 5*C*). $SMV_{segmental\ BI}$ (26,031.4 ± 3,312.2 cm^3) did not significantly differ from SMV_{MRI} (26,738.3 ± 3,120.8 cm^3), but $SMV_{whole\ body\ BI}$ (27,498.3 ± 3,694.3 cm^3) was significantly greater (Fig. 6). Consequently, the data obtained by the whole body BI analysis were omitted from the analysis for developing the prediction equation using the pooled data.

Prediction equation derived from the pooled data. In the pooled data, too, the BI indexes of the upper leg and trunk were selected as significant contributors to predict SMV_{MRI} and produced an equation, $SMV_{segmental\ BI} = 116.1 \times [(L_{TR})^2/Z_{TRwhole} + 1{,}220.8 \times (L_{upper\ leg})^2/Z_{upper\ leg}] - 4{,}913.1$, with R^2 and SEE values of 0.842 and 1,693.8 cm^3 (6.1%), respectively. The relative contribution of two BI indexes to the prediction of the SMV_{MRI} was 52.6% for the upper leg and 32.8% for the trunk. The regression analysis indicated that the slope and intercept of the regression equation for the relationship between SMV_{MRI} and $SMV_{segmental\ BI}$ were not significantly different from 1 and 0, respectively (Fig. 7*A*). There was no significant difference between SMV_{MRI} and SMV_{BI}. In addition, no significant systematic error (r = 0.239, NS) was found in the Bland-Altman plot (Fig. 7*B*).

DISCUSSION

The present study is the first to compare the accuracy of SMV_{BI} between whole body and segmental BI analyses. In the validation group, the whole body and segmental BI analyses produced equations with a similar accuracy for estimating SMV_{MRI}. In the cross-validation group, however, $SMV_{whole\ body\ BI}$ was significantly greater than SMV_{MRI}, and

Table 2. *Descriptive data on MRI-measured skeletal muscle volume of subjects*

	Validation Group (n = 20)		Cross-Validation Group (n = 10)		Total (n = 30)	
Variables	Mean	SD	Mean	SD	Mean	SD
Skeletal muscle volume, cm^3						
Whole body	28,429	5,256	26,451	3,077	27,770	4,684
Upper arm	2,642	565	2,482	601	2,589	572
Lower arm	1,349	350	1,283	265	1,327	321
Upper leg	9,542	1,964	9,107	1,213	9,397	1,740
Lower leg	2,946	505	3,062	524	2,985	505
Trunk	11,950	2,256	10,518	1,259	11,472	2,073

n = no. of men/group.

Table 3. *Descriptive data on Z values and BI indexes of subjects*

Variables	Validation Group (n = 20)		Cross-Validation Group (n = 10)		Total (n = 30)	
	Mean	SD	Mean	SD	Mean	SD
Z value, Ω						
Whole body BI analysis						
$Z_{whole\ body}$	447.0	61.7	454.0	61.4	449.3	60.6
Segmental BI analysis						
$Z_{upper\ arm}$ (right side)	75.1	13.9	79.5	15.1	76.5	14.2
$Z_{upper\ arm}$ (left side)	73.9	15.0	78.7	14.7	75.5	14.9
$Z_{lower\ arm}$ (right side)	117.7	19.0	119.3	20.8	118.3	19.3
$Z_{lower\ arm}$ (left side)	120.4	19.7	121.0	20.9	120.6	19.8
$Z_{upper\ leg}$ (right side)	51.7	7.5	53.4	6.3	52.3	7.1
$Z_{upper\ leg}$ (left side)	51.2	7.2	53.3	8.1	51.9	7.5
$Z_{lower\ leg}$ (right side)	141.5	10.3	140.0	18.0	141.6	18.6
$Z_{lower\ leg}$ (left side)	142.2	21.0	143.5	17.8	142.7	19.7
$Z_{TRwhole}$	33.2	21.0	33.7	3.0	33.3	3.7
BI index, cm^2/Ω						
Whole body BI analysis						
$Height^2/Z_{whole\ body}$	70.2	11.0	67.8	8.7	69.4	10.2
Segmental BI analysis						
$(L_{upper\ arm})^2/Z_{upper\ arm}$	7.7	1.6	7.1	1.7	7.5	1.7
$(L_{lower\ arm})^2/Z_{lower\ arm}$	2.6	0.5	2.5	0.4	2.5	0.5
$(L_{upper\ leg})^2/Z_{upper\ leg}$	16.5	2.6	15.9	1.8	16.3	2.4
$(L_{lower\ leg})^2/Z_{lower\ leg}$	5.9	0.9	5.8	0.6	5.8	0.8
$(L_{TR})^2/Z_{TRwhole}$	114.2	18.0	102.1	13.3	110.2	17.4

n = no. of men/group. BI, bioelectrical impedance; Z, measured BI; L, segment length; TR, trunk.

so only the segmental BI analysis was cross-validated. The SEE value (6.3%) obtained from the application of the segmental BI analysis to the pooled data was lower than that (9%) reported in a prior study (14) that used the whole body BI analysis to estimate whole body SM mass. The present results indicated that the segmental BI analysis could predict SMV_{MRI} more accurately than the whole body BI analysis.

Janssen et al. (14) reported that the prediction equation derived from data on Caucasians obtained using the whole body BI analysis overestimated the whole body SM mass in an Asian cohort. They speculated that the biological differences between Caucasians and Asians would influence the relationship between Z value and the whole body SM mass. Meanwhile, the present study indicated that the whole body BI analysis overestimated SMV_{MRI} even though Asians were used as the subjects to develop the prediction equation. Certainly, there is a possibility that the poor performance of the whole body BI analysis in the cross-validation group might be attributed to the subject sample size. However, if the volume units are converted to mass units by multiplying the volumes by the assumed constant density for adipose-free SM (1.04 kg/l) (20), one can find a similar average value (27.5 ± 5.9 kg) for the subjects in the present study as that (26.4 ± 7.6 kg) examined by Janssen et al. (14). Regardless of the subject sample size taken in the present study, therefore, it seems that the whole body BI analysis itself has a potential to overestimate SMV_{MRI}.

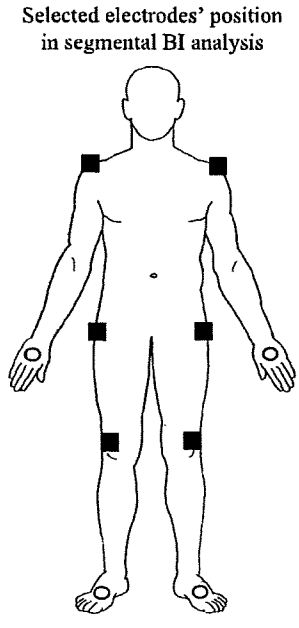

Fig. 3. Selected electrode positions in the segmental BI analysis.

A prior study (12) suggested that the application of the whole body BI analysis to the estimation of the lean body mass did not reflect the relative development of lean tissue mass in the upper arms and upper legs within the arms and legs, respectively, to the BI measurements. In general, SM volume is less in the distal than the proximal segment in each of the arms and legs. From the findings of Kanehisa and Fukunaga (15), the SM CSA of the upper leg was greater in the strength-trained athletes than in the untrained subjects, but that of the lower leg was similar between the two groups, when the difference in lean body mass was normalized. In the subject sample including athletes, therefore, it was expected that the relative difference in the SM volume between the segments in either arms or legs would be a factor explaining the residual of the whole body BI analysis. In the pooled data of the present study, however, there were no significant relationships between the

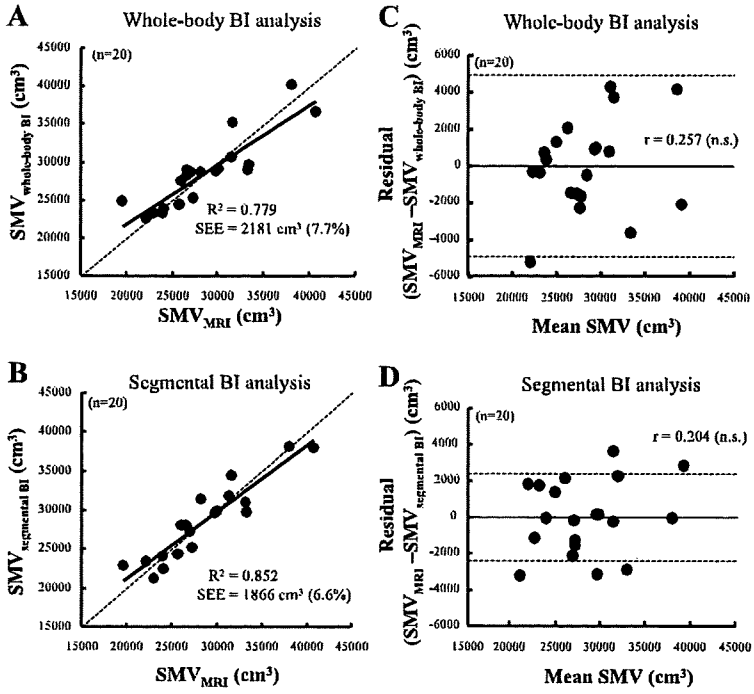

Fig. 4. Relationship between the measured skeletal muscle volume (SMV_{MRI}) and estimated SMV (*A* and *B*) and between the residual (difference between the measured and estimated SMV) and mean SMV determined by 2 methods (*C* and *D*) in the validation group. *A* and *C* indicate the corresponding relationship for the whole body BI analysis, and *B* and *D* for the segmental BI analysis. SEE, SE of estimate. Solid lines, regression lines. Dashed lines in *A* and *B* are lines of identity. Horizontal dashed lines in *C* and *D* are lines of ±2SD.

residual of the whole body BI analysis and the SM volume ratios of the upper arm to the arm ($r = -0.117$, NS) and the upper leg to the leg ($r = 0.271$, NS). This implies that the accuracy of the whole body BI analysis in the estimates of SMV_{MRI} was independent of the differences in SM distribution between the proximal and distal parts in each of the upper and lower extremities. On the other hand, the percentage of the sum of SM volumes of the upper arm, upper leg, and trunk to the SMV_{MRI} was 84.4%. Compared with the SM CSAs and volumes of these segments, those of the lower arm and lower leg were considerably smaller as shown in Fig. 2 and Table 2. Therefore, if the *Z* value measured by the whole body BI analysis would reflect the SM volume of these distal segments rather than that of the upper arm, upper leg, and trunk, it might

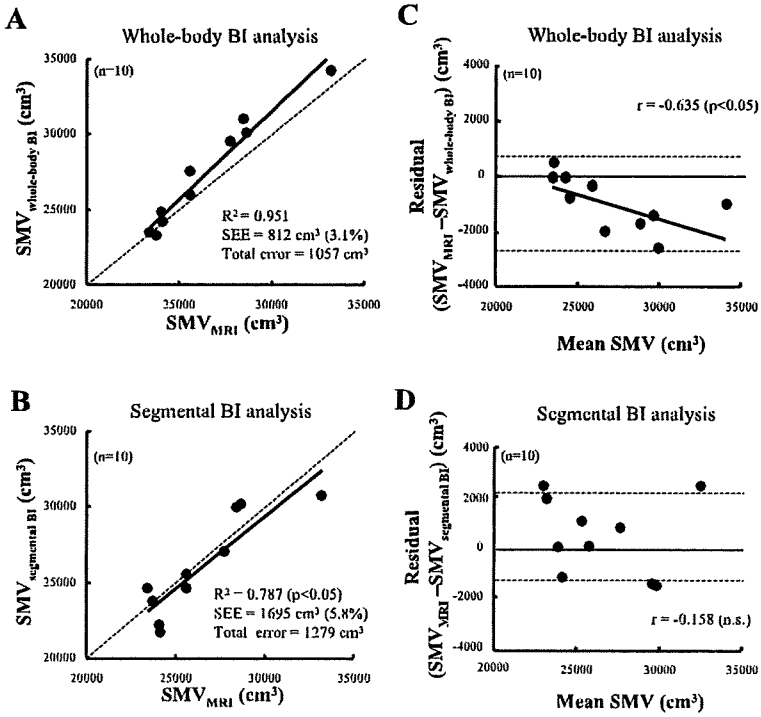

Fig. 5. Relationship between measured and estimated SMV (*A* and *B*) and between the residual (difference between the measured and estimated SMV) and mean SMV determined by 2 methods (*C* and *D*) in the cross-validation group. *A* and *C* indicate the corresponding relationship for the whole body BI analysis, and *B* and *D* for the segmental BI analysis. Solid lines: regression lines. Dashed lines in *A* and *B* are lines of identity. Horizontal dashed lines in *C* and *D* are lines of ±2SD.

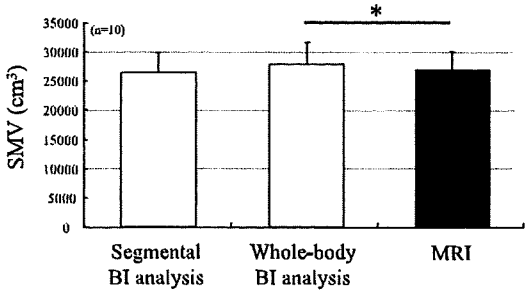

Fig. 6. Measured and estimated SMV in both BI analyses. *Significantly different from MRI.

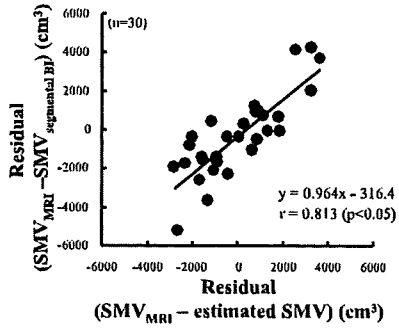

Fig. 8. Relationship between the residuals (difference between the measured and estimated SMV) in the predicting equation using the BI indexes of the lower arm and lower leg as independent variables (*y*-axis) and in the whole body BI analysis (*x*-axis) with the pooled data. Solid line, regression line.

be a reason why the predicting equation was not cross-validated.

To test the assumption mentioned above, we applied a multiple regression analysis using the whole body BI value as the dependent variable and the BI values in the upper arm, lower arm, upper leg, lower leg, and trunk as the independent variables in the pooled data. As a consequence, the relative contribution of the BI values in the lower arm and lower leg for determining the whole body BI was 60.0%. In addition, the residual in the estimate of SMV_{MRI} using the BI indexes of the lower arm and lower leg as the independent variables was significantly correlated with that of the whole body BI analysis ($r = 0.831$, $P < 0.05$) in the pooled data (Fig. 8). These results indicate that the whole body BI value is largely influenced by the distal extremities, and consequently it may be a factor producing the error in the estimate of SMV_{MRI} by the whole body BI analysis. On the other hand, it may be that the segmental BI analysis used in the present study resulted in a higher accuracy for estimating SMV_{MRI} compared with the whole body BI analysis by selecting the BI indexes of the upper leg and trunk, which have higher percentages of the SM volume in the whole body (33.8% and 41.3%, respectively, in the pooled data).

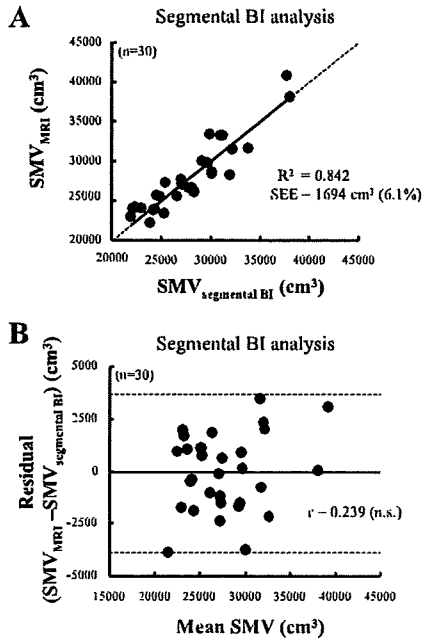

Fig. 7. Relationship between the measured and estimated SMV (*A*) and between the residual (difference between the measured and estimated SMV) and mean SMV determined by 2 methods (*B*) with the pooled data. Both indicate the corresponding relationship for the segmental BI analysis. Solid line, regression line. Dashed line in *A* is line of identity. Horizontal dashed lines in *B* are lines of ±2SD.

From the finding of Ishiguro et al. (12), the BI indexes of the upper arm, upper leg, and trunk were selected for estimating the lean body mass by segmental BI analyses. At the start of the present study, it seemed that the BI index of the upper arm would also be a significant contributor for predicting the whole body SM volume. However, the present results indicated that SMV_{MRI} could be predicted by measuring the BI indexes of the trunk and upper leg only. Adding the BI index of the upper arm as a predictive variable did not improve the accuracy of the estimates of SM volume. One reason for this result may be the procedure used for measuring the trunk *Z* values. The present study measured the *Z* values of the trunk in five regions (both sides of the upper region, the middle region, and both sides of the lower region). On the other hand, Ishiguro et al. (13) assumed the trunk to be one cylinder and obtained the *Z* value using a network circuit model with the detector electrodes on both sides of knee and elbow. In their results, the contribution of the trunk BI index for predicting lean body mass was only 7.1%. This value was considerably different from the substantial percentage of the trunk lean tissue mass to that of the whole body, ~50% (19). We cannot directly compare the contribution of the trunk BI index of the present study to that of the prior study (12) because the reference value (SMV_{MRI} vs. the lean body mass) and the subjects are different. In the present results, however, the contribution of the trunk BI index [$(L_{TR})^2/Z_{TRwhole}$] indicated a relatively high (32.8%) and closer value to the average in the percentage of the trunk SM volume (41.3 ± 2.7%) to SMV_{MRI} in the pooled data. On the other hand, the percentage of the upper arm SM volume to the SMV_{MRI} was lower (9.3 ± 1.0%) than that of upper leg (33.8 ± 1.9%) and trunk. The SM volume in the upper arm was significantly correlated to that of the trunk ($r = 0.888$, $P < 0.05$) and the upper leg ($r = 0.816$, $P < 0.05$). Therefore, it may be assumed that the application of the electrode placements that enabled us to obtain *Z* values from the five regions of the trunk improved the contribution of the trunk BI index for estimating SMV_{MRI} and eliminated the need to enter the upper

arm BI index into the prediction equation as the predictive variable.

In estimating the trunk SM volume from the segmental BI analysis, however, the influence of the visceral tissue volume on the accuracy cannot be excluded. Particularly, the visceral tissue volume at 41–50% L_{TR}, which has high conductivity because it is mainly made up of smooth muscle and water, has a low but significant negative correlation between the residual of the trunk SM volume estimates, expressed as a percentage of the trunk SM volume (13). Meanwhile, a regression analysis for the pooled data of this study indicated that the residual of SMV_{MRI} in the segmental BI analysis did not significantly correlate to the percentage of the visceral tissue volume to the SM volume in each part of the trunk ($r = -0.259$ to 0.011, NS). In contrast to the relatively high percentage of the visceral tissue volume to the total tissue volume (31.0%) in the trunk (13), the corresponding value is 7.1% of the whole body in the pooled data. This relatively low percentage might be assumed to have less influence on the accuracy of the SMV_{MRI} estimation. However, the subjects examined here were healthy young men. With regard to the influence of visceral tissue volume on the estimate of the whole body SM, further investigation using obese and/or elderly individuals is needed.

Before summarizing the present results, we should comment on the limitations of the experimental design in the present study. The sample size was relatively small. Also, only young adult males were examined. In general, the distribution of the SM of females differs from that of males (1). Moreover, the accuracy of the predicting body composition from BI analysis is influenced by the body fat percentage (4) and age (3). Hence, we cannot deny that the accuracy of the equation developed in the present study would vary when subject samples involving females, obesity, and/or elderly are taken for analysis. In addition, the method used to analyze the MRI scans for regional areas was a bit primitive and did not exploit more advanced segmentation software being used in this research field. There remains a possibility that smaller islands of adipose tissue within the skeletal muscle bundle are not fully excluded, as they would be using newer approaches, and so the SM volume might be overestimated. Especially, the use of the software would be heightened to examine the elderly, because they have three times higher accumulation of the intramuscular fat compared with the young men (11). Further study, to clarify the influences of differences in the subject samples and the method used to analyze the MRI scans on the estimate of SM volume, is needed to generalize the findings obtained in the present study.

In summary, the findings obtained here indicated that the validity and cross-validity of the segmental BI analysis that measures Z values from both sides of the upper arm and upper leg, and five regions (both sides of the upper, the middle, and both sides of the lower region) of the trunk was confirmed. On the other hand, the whole body BI analysis significantly overestimated the whole body SM volume. The development of segmental BI technique predicting the whole body SM volume will be of benefit to lean, obese, or long-term hospitalized individuals as well as athletes for evaluating conventionally their own muscularity.

REFERENCES

1. **Abe T, Kearns CF, Fukunaga T.** Sex differences in whole body skeletal muscle mass measured by magnetic resonance imaging and its distribution in young Japanese adults. *Br J Sports Med* 37: 436–440, 2003.
2. **Bartok C, Schoeller DA.** Estimation of segmental muscle volume by bioelectrical impedance spectroscopy. *J Appl Physiol* 96: 161–166, 2004.
3. **Baumgartner RN.** Electrical impedance and total body electrical conductivity. In: *Human Body Composition*, edited by Roche AF, Heymsfield AB, Lohman TG. Champagne, IL: Human Kinetics, 1996.
4. **Baumgartner RN, Ross R, Heymsfield SB.** Does adipose tissue influence bioelectric impedance in obese men and women? *J Appl Physiol* 84: 257–262, 1998.
5. **Baumgartner RN, Chumlea WC, Roche AF.** Estimation of body composition from bioelectric impedance of body segments. *Am J Clin Nutr* 50: 221–226, 1989.
6. **Bland JM, Altman DG.** Statistical methods for assessing agreement between two methods of clinical measurement. *Lancet* 1: 307–310, 1986.
7. **Bracco D, Thiebaud D, Chiolero RL, Landry M, Burckhardt P, Schutz Y.** Segmental body composition assessed by bioelectrical impedance analysis and DEXA in humans. *J Appl Physiol* 81: 2580–2587, 1996.
8. **Caton JR, Mole PA, Adams WC, Heustis DS.** Body composition analysis by bioelectrical impedance: effect of skin temperature. *Med Sci Sports Exerc* 20: 489–491, 1988.
9. **Foster KR, Lukaski HC.** Whole body impedance: What does it measure? *Am J Clin Nutr* 64, *Suppl* 3: 388S–396S, 1996.
10. **Fuller NJ, Elia M.** Potential use of bioelectrical impedance of the "whole body" and of body segments for the assessment of body composition: comparison with densitometry and anthropometry. *Eur J Clin Nutr* 43: 779–791, 1989.
11. **Kent-Braun JA, Ng AV, Young K.** Skeletal muscle contractile and noncontractile components in young and older women and men. *J Appl Physiol* 88: 662–668, 2000.
12. **Ishiguro N, Kanaehisa H, Miyatani M, Masuo Y, Fukunaga T.** A comparison among three bioelectrical impedance analyses for predicting lean body mass in a population with a large difference in muscularity. *Eur J Appl Physiol* 94: 25–35, 2005.
13. **Ishiguro N, Kanaehisa H, Miyatani M, Masuo Y, Fukunaga T.** Applicability of segmental bioelectrical impedance analysis for predicting trunk skeletal muscle volume. *J Appl Physiol* 100: 572–578, 2006.
14. **Janssen I, Heymsfield SB, Baumgartner RN, Ross R.** Estimation of skeletal muscle mass by bioelectrical impedance analysis. *J Appl Physiol* 89: 465–471, 2000.
15. **Kanehisa H, Fukunaga T.** Profiles of musculoskeletal development in limbs of college Olympic weightlifters and wrestlers. *Eur J Appl Physiol Occup Physiol* 79: 414–420, 1999.
16. **Lukaski HC.** Estimation of muscle mass. *Human Body Composition*, edited by Roche AF, Heymsfield SB, Lohman TG. Champaign, IL: Human Kinetics, 1996.
17. **Miyatani M, Kanehisa H, Fukunaga T.** Validity of bioelectrical impedance and ultrasonographic methods for estimating the muscle volume of the upper arm. *Eur J Appl Physiol* 82: 391–396, 2000.
18. **Miyatani M, Kanehisa H, Masuo Y, Ito M, Fukunaga T.** Validity of estimating limb muscle volume by bioelectrical impedance. *J Appl Physiol* 91: 386–394, 2001.
19. **Organ LW, Bradham GB, Gore DT, Lozier SL.** Segmental bioelectrical impedance analysis: theory and application of a new technique. *J Appl Physiol* 77: 98–112, 1994.
20. **Snyder WS, Cooke MJ, Manssett ES, Larhansen LT, Howells GP, Tipson IH.** *Report of the Task Group on Reference Man.* Oxford, UK: Pergamon, 1975.

Available online at www.sciencedirect.com
ScienceDirect
Neuroscience Letters 422 (2007) 202–206
Neuroscience Letters
www.elsevier.com/locate/neulet

Larger center of pressure minus center of gravity in the elderly induces larger body acceleration during quiet standing

Kei Masani [a,b,*], Albert H. Vette [a,b], Motoki Kouzaki [c], Hiroaki Kanehisa [c], Tetsuo Fukunaga [d], Milos R. Popovic [a,b]

[a] *Rehabilitation Engineering Laboratory, Institute of Biomaterials and Biomedical Engineering, University of Toronto, Canada*
[b] *Rehabilitation Engineering Laboratory, Lyndhurst Centre, Toronto Rehab, Canada*
[c] *Graduate School of Human and Environmental Studies, Kyoto University, Japan*
[d] *School of Sports Sciences, Waseda University, Japan*

Received 17 January 2007; received in revised form 10 June 2007; accepted 12 June 2007

Abstract

When an inverted pendulum approximates quiet standing, it is assumed that the distance between the center of pressure and the vertical projection of the center of mass on the ground (COP–COG) reflects the relationship between the controlling and controlled variables of the balance control mechanism, and that the center of mass acceleration (ACC) is proportional to COP–COG. As aging affects the control mechanism of balance during quiet standing, COP–COG must be influenced by aging and, as a result, ACC is influenced by aging as well. The purpose of this study was to test the hypotheses that aging results in an increased COP–COG amplitude and, as a consequence, that ACC becomes larger in the elderly than the young. Fifteen elderly and 11 young subjects stood quietly on a force platform with their eyes open or closed. We found that (1) the standard deviations of COP–COG and ACC were larger in the elderly than in the young, irrespective of the eye condition; (2) COP–COG is proportional to ACC in both age groups, i.e., the inverted pendulum assumption holds true for quiet standing. The results suggest that a change in the control strategy that is due to aging causes a larger COP–COG in the elderly and, as a consequence, that ACC becomes larger as well.

Keywords: Standing; Equilibrium; Center of pressure; Center of mass; Center of gravity

Since the human body is inherently unstable, a control system is required to stabilize the body even during quiet standing. Active control provided by the central nervous system as well as passive mechanical stabilization contribute to stabilizing the body [17,18,22,24,27,28]. Age-related changes in the central nervous system and the musculoskeletal system can influence various functions of this control mechanism, and, as a result, can reduce postural stability [12,21]. Such age-related changes in postural stability during quiet standing have been investigated using time-varying characteristics of the center of pressure (COP) and/or the center of mass (COM) [2,8,11,19,20,25,26,29]. These measures have been associated with falling in the elderly [19,20], which is one of the serious health problems related to aging.

Frequently used measures are the statistical measures of COP and COM in the time domain, such as their standard deviation or mean velocity, or in the frequency domain, such as their total power or the median frequencies [11,13,29,30]. Several studies have focused on the association between COP and the vertical projection of COM (COG), using the distance between COP and COG (COP–COG) as the variable that provides a good assessment of spontaneous sway during quiet standing [3–7,31,32,1]. Corriveau et al. reported that the root mean square of COP–COG is larger in the elderly who have neurological impairments [3] as well as in stroke patients [5] when compared to healthy elderly individuals. They also discovered that physiological factors, such as peripheral somatosensory input and muscle strength, influence the amplitude of COP–COG in healthy elderly individuals and the elderly with neurological impairments [6]. These studies suggest that a neurological impairment pertaining to the control of quiet standing enlarges the COP–COG amplitude.

COP–COG is the variable that reflects the relationship between the controlling and controlled variables in the con-

* Corresponding author at: Rehabilitation Engineering Laboratory, Lyndhurst Centre, Toronto Rehab, 520 Sutherland Drive, Toronto, Ont. M4G3V9, Canada. Tel.: +1 416 597 3422x6213; fax: +1 416 425 9923.
E-mail address: k.masani@utoronto.ca (K. Masani).

0304-3940/$ – see front matter © 2007 Elsevier Ireland Ltd. All rights reserved.
doi:10.1016/j.neulet.2007.06.019

trol mechanism of quiet standing when approximated using an inverted pendulum model. If human posture during quiet standing can be approximated by an inverted pendulum, the equation of motion is described as

$$I\ddot{\theta} = mgh \sin\theta - T, \quad (1)$$

where m is the mass of the body without the feet, g the gravitational acceleration coefficient, h the distance between COM and the ankle joint, I the moment of inertia of the body about the ankle joint, θ the body angle to the vertical axis, $\ddot{\theta}$ the body angular acceleration, and T is the ankle torque produced by the subject about the ankle joint. From the view of the control mechanism, T is the controlling variable, whereas θ is the controlled variable. Assuming that the body sway amplitude is small, $T \approx mg\mathrm{COP}$ and $mgh\sin\theta = mg\mathrm{COG}$. Therefore, COP is approximately proportional to the controlling variable, and COG is also approximately proportional to the controlled variable since $\sin\theta \approx \theta$ for small angles. Since the relationship between the controlling and controlled variables is sensitive to changes in the control system, it is assumed that COP–COG is sensitive to the change of the control system. As such, the above-mentioned previous studies imply that the increment of COP–COG is due to the alteration of the control strategy caused by the neurological impairments. However, only a few studies to date have compared COP–COG between the healthy elderly and the young. Accordingly, we suggest in the present study that a potential hypofunction of the motor control strategy due to aging could be detectable by this measure.

The right-hand side of Eq. (1) can be rewritten as $-mg$(COP–COG). Then, considering an additional approximation of $\ddot{\theta} \approx \ddot{COM}/h = \mathrm{ACC}/h$, one can derive

$$\mathrm{COP} - \mathrm{COG} = -\frac{I}{mgh}\mathrm{ACC} \quad (2)$$

where ACC is the horizontal COM acceleration [34]. Eq. (2) expresses that COP–COG is proportional to ACC. Therefore, if COP–COG is enlarged by the alteration of the control strategy due to aging, the increment of the COP–COG amplitude will result in an increment of the ACC amplitude.

The purpose of this study was to test the hypotheses that aging results in an increased COP–COG amplitude and, as a consequence, that ACC becomes larger in the elderly than the young.

Fifteen healthy elderly male subjects (72.7 ± 5.6 years, mean ± S.D. age) and 11 healthy young male subjects (29.0 ± 7.7 years) participated in this study. At the time of the experiments, the subjects reported having no neurological or musculoskeletal impairments, and were living independently in the community. All subjects gave written informed consent according to the principles of the Declaration of Helsinki, which was approved by the local ethical committee. Each subject was asked to maintain a quiet stance posture standing barefoot with eyes open (EO) and closed (EC). The subjects had their arms hanging along the sides of their body, their feet were parallel and the distance between their heels was 15 cm. One trial was performed for each visual condition. The order of application of EO and EC conditions was randomized among the subjects. The duration of each trial was approximately 70 s, and data from the latter 60 s were subjected to subsequent analyses. A sufficient resting time was allowed between trials. Note that we focused only on the anterior–posterior direction of sway in this study. A force platform (Type 9281B, Kistler, Switzerland) was used to measure the subjects' COP displacement and the horizontal ground reaction force during quiet standing. All data were sampled at 1 kHz using a 16 bit analog-to-digital converter (PowerLab, ADInstruments, New Zealand). The anthropometric estimation of body dimensions was based on Ref. [33]: $h = 0.547H$, where H indicates the subject's height; $m = 0.971M$, where M indicates the subject's body mass; $I = 0.319MH^2$.

To obtain the COM displacement, we adopted the *zero-point-to-zero-point double integration technique* or *gravity line projection method*. This method has initially been proposed by King and Zatsiorsky [15] and has been described in more detail in a later work [35]. It is based on the premise that COP and COG coincide when ACC, calculated using the horizontal force, is equal to zero. Using this premise, we were able to obtain the discrete COG at the instances when ACC was equal to zero. These discrete COG points were connected by calculating the double integral of ACC obtained via the horizontal force. For this analysis, all kinematic and kinetic data were low-pass filtered using a fourth-ordered, zero-phase-lag Butterworth filter [33] with a cutoff frequency of 10 Hz according to [16]. COP–COG was calculated using the COP and COG time series. ACC was calculated using the horizontal force time series, i.e., $\mathrm{ACC} = f_h/m$. We quantified the fluctuation amplitude of all variables using the standard deviation (S.D.) for each trial. The S.D.s of COP, COG, ACC, and COP–COG were used in the subsequent statistical analysis. We also tested how well ACC, estimated from COP–COG using Eq. (2), corresponded to the actual ACC obtained in the experiments. Linear regression analysis was used to evaluate the relationship between the S.D. of the actual ACC and the S.D. of the ACC estimated from COP–COG. In the regression analysis, the data from EO and EC were pooled, while the regression analysis was done separately for each age group. The effects of age and eye conditions were analyzed using two-way repeated measures ANOVA with a within-subject factor of eye condition and a between-subject factor of age for each variable. $P < 0.05$ was used as a level of significance to prevent excessive false-positive results.

Fig. 1 shows examples of COP, COG, COP–COG, and ACC data for a young subject (left panel) and an elderly subject (right panel) for the EC condition. Note that only 15 s of data out of the analyzed 60 s are presented in the figure to isolate the signal features. The features of COP and COG resembled each other closely. However, the COP was slightly larger than COG as it fluctuated around COG. The features of COP–COG resembled the inverse form of ACC well. Comparing the data between the young and elderly subjects, one can see that the COG amplitude seemed similar, whereas COP showed a larger deviation from COG in the elderly than in the young. The larger deviation in the elderly became more evident when the time series of COP–COG and ACC were compared between the age groups: Both time series appeared distinctly larger in the elderly than in the young.

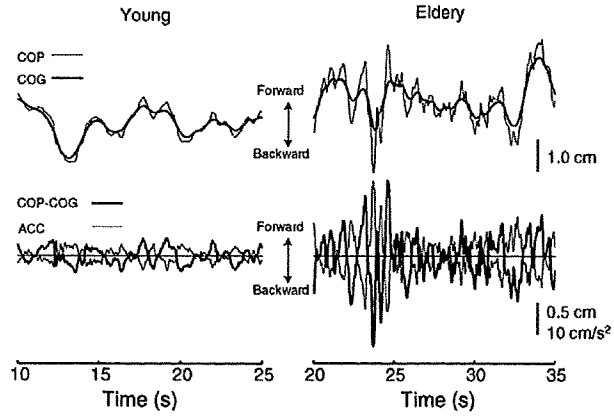

Fig. 1. Representative example time series of COP, COG, COP–COG, and ACC for a young subject (left panel) and an elderly subject (right panel) for EC condition.

Fig. 2 shows group mean values of S.D. of COP, COG, ACC, and COP–COG for each age group and eye condition. COP was significantly larger for the EC than in the EO condition ($P=0.015$), while there was no significant difference between age groups ($P=0.478$). There was no interaction between the factors age group and eye condition for COP ($P=0.702$). For COG, there was no significant difference between eye conditions ($P=0.079$) and between age groups ($P=0.834$). ACC was significantly larger in the elderly than in the young ($P=0.003$) and significantly larger for the EC than in the EO condition ($P<0.0001$). There was no interaction between the factors age group and eye condition for ACC ($P=0.055$). COP–COG was significantly larger in the elderly than in the young ($P=0.007$), and significantly larger for the EC than in the EO condition ($P<0.0001$). There was no interaction between the factors age group and eye condition for COP–COG ($P=0.062$).

We compared the actual ACC determined from f_h with the ACC estimated from COP–COG in Fig. 3 for each age group. Linear regression analysis provided the regression lines of: $Y=-0.21+1.14X$, $R=0.973$ for the young, and $Y=-0.04+1.01X$, $R=0.976$ for the elderly (X indicates the actual ACC, and Y indicates the estimated ACC). For the young group, the 95% confidence intervals for the slope and intercept were from 1.01 to 1.26 and from −0.34 to −0.07, respectively. For the elderly group, the 95% confidence intervals for the slope and intercept were from 0.93 to 1.10 and from −0.20 to 0.93, respectively. The confidence interval of the regression line of the elderly group included the line of identity, while that of the young group did not. However, note that their line was also fairly close to the line of identity despite considerable errors in the estimation of the anthropometric parameters. Thus, the result suggests that the actual ACC corresponds to the value estimated from COP–COG using the inverted pendulum model.

We clearly demonstrated that both COP–COG and ACC are larger in the elderly than in the young irrespective of the eye condition. Since the standard deviation of the ACC fluctuation matches the one estimated from COP–COG using an inverted pendulum model, the inverted pendulum assumption was validated for the quiet standing condition in this experiment. Thus, we demonstrated that COP–COG is larger in the elderly than in the young, and, as a consequence, ACC is larger as well.

COP is proportional to the ankle torque, which is regulated by the central nervous system to restore the equilibrium of balance. COP can therefore be interpreted as the *controlling* variable of the postural control system. COM on the other hand is an imaginary point at which the total body mass can be assumed to be concentrated. The position of the COM has been hypothesized to be subject to body postural control, which is the *controlled* variable of the system. Thus, postural control during quiet stance

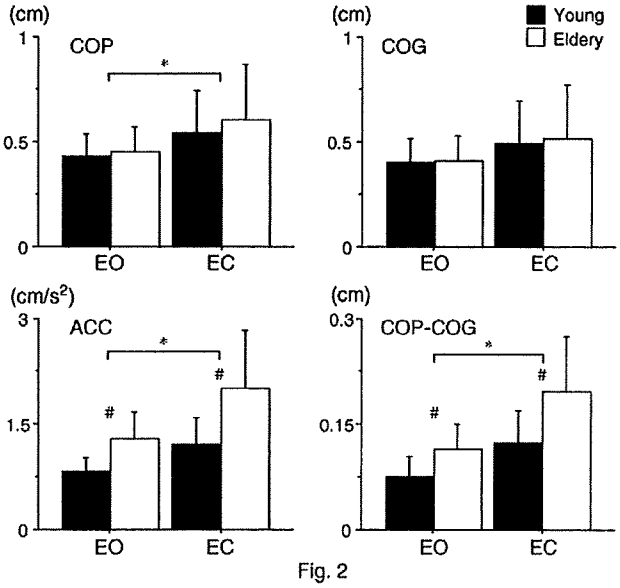

Fig. 2

Fig. 2. Group mean values of S.D. of COP (left upper panel), COG (right upper panel), ACC (left lower panel), and COP–COG (right lower panel) for each age group and eye condition. White bar indicates elderly group and black bar indicates young group. EO and EC indicate the eyes open and the eyes closed conditions, respectively. Data are group means ± standard deviations. #$P<0.05$ between age groups. *$P<0.05$ between eye conditions.

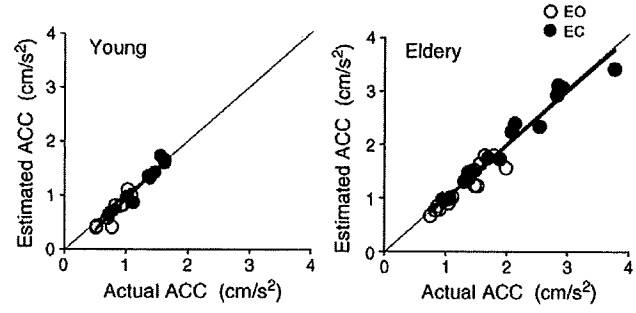

Fig. 3. Comparison between the actual ACC and the estimated ACC from COP–COG for each trial. Open circle indicates EO condition, and closed circle indicates EC condition. Left panel shows plots for young subjects, and right panel shows that of elderly subjects. The bold line indicates the regression line for each age group. Linear regression analysis provided the regression lines of: $Y=-0.21+1.14X$, $R=0.973$ for the young, and $Y=-0.04+1.01X$, $R=0.976$ for the elderly (X indicates the actual ACC, and Y indicates the estimated ACC). The plots for EO and EC conditions were grouped together when calculating the regression line for each age group. Note that regression lines (thick lines) are close to the lines of identity (thin lines) in both age groups.

can be characterized by the relation between the COP and the COM. Since the relationship between these controlling and controlled variables is sensitive to changes in the control system, it is assumed that also COP–COM is sensitive to such changes. Thus, the identified increase in COP–COG in the elderly strongly suggests a change in the control strategy that is due to aging.

At this stage, the age-related change in the physiological control system that is actually responsible for the present findings cannot be entirely captured. One explanation of the underlying mechanisms may be the following: Maurer and Peterka [23] demonstrated in their theoretical study that higher gain controllers or a higher driving noise level can account for the change of COP measures in aging. They simplified the postural control system using a continuous feedback strategy [28], in which various sensory modalities of the physiological system are integrated, yielding an estimate of the COM angle. The neural control center in their study is approximated as a PID (proportional, integral, and derivative) controller that generated the desired ankle torque. A higher gain controller, i.e., a PID controller with larger gains, represents a neural control system that generates a large response to a certain amount of sway, which results in an overreacting system in the extreme case. Thus, they suggested that the elderly show a larger response to a certain amount of sway compared to the young. Since a higher gain controller is generally supposed to create a larger deviation of the controlling variable from the controlled variable, our result that COP–COG is larger in the elderly may imply this age-related change in the control strategy. A higher driving noise level represents a larger amount of internal disturbance torque that might be due to respiration, the heart beat, and the error in the motor command. Thus, also an increase in the driving noise level could cause a larger deviation between the controlling and controlled variables. Therefore, the current result may reflect the same change in the control strategy as in Maurer and Peterka [23], implying higher gain controllers or a higher driving noise level in the elderly. Further investigation is required to fully understand the underlying mechanisms.

To date, one study demonstrated that COP–COG is larger in the elderly than in the young [1]. They compared the measure among the young of age 22.9 ± 4.0 years (Y-group), the elderly of age 69.2 ± 2.4 years (S-group), and the elderly of age 81.2 ± 6.3 years (E-group). They reported that the root mean square of COP–COG in the anterior–posterior direction, which is equivalent to the standard deviation adopted in this study, is larger in the E-group than in the Y-group, while COP–COG is identical between the S-group and the Y-group. They also reported that the root mean square of COG is identical among the groups. Our elderly subjects were situated between their S-group and E-group, i.e., a t-test revealed that our elderly subjects were significantly older than their S-group, and significantly younger than their E-group ($P < 0.05$ in both tests). Thus, it is plausible that our elderly subjects showed a similar behavior as the E-group in their study, i.e., that COP–COG is larger than for the young subjects and COG is identical between the age groups. Although they used a different method to calculate COG [31,32] and tested only the EO condition, our results agree with their finding.

We also demonstrated that the larger COP–COG accounts for the larger ACC in the elderly by validating the inverted pendulum assumption, whereas Berger et al. [1] did not. In literature, it has been investigated several times to which extent the inverted pendulum assumption fits the quiet standing posture [9,10,14]. Karlsson and Lanshammar [14] demonstrated that up to 90% of the standard deviation of the COM acceleration was accounted for by the inverted pendulum model. In the present study, we also demonstrated that the standard deviation of ACC was accounted for by the standard deviation of COP–COG. The result suggests that ACC during quiet standing was caused by COP–COG following the equation of motion of the inverted pendulum.

In the literature, many measures of spontaneous sway during quiet standing have been proposed. Several measures such as the mean velocity successfully distinguished the properties of the elderly and young [29]. However, these measures only provide a *parametric* description of the spontaneous sway and do not reflect specific physiological characteristics of the control system. As such, it is still important to investigate alternative force plate measures that can capture characteristics of spontaneous sway in the elderly, which are closely tied to the actual control system. Both COP–COG and ACC are such measures since they distinguish changes of postural sway in aging and at the same time have physiological meanings.

In conclusion, we found that (1) the standard deviations of COP–COG and ACC were larger in the elderly than in the young, irrespective of the eye condition; (2) COP–COG is proportional to ACC in both age groups, i.e., the inverted pendulum assumption holds true for quiet standing. The results suggest that a change in the control strategy that is due to aging causes a larger COP–COG in the elderly and, as a consequence, that ACC becomes larger as well.

Acknowledgements

We are grateful to Xavier Tortolero for his helpful discussion. We also thank Ms. Zina Bezruk for her assistance with the manuscript preparation. This work was supported by Casio Scientific Foundation; Nihon Kenko Kaihatsu Foundation; Foundation for Life Science and Moritani Scholarship Foundation; Defence Research and Development Canada, Toronto Branch.

References

[1] L. Berger, M. Chuzel, G. Buisson, P. Rougier, Undisturbed upright stance control in the elderly: Part 1. Age-related changes in undisturbed upright stance control, J. Mot. Behav. 37 (2005) 348–358.
[2] J.J. Collins, C.J. De Luca, A. Burrows, L.A. Lipsitz, Age-related changes in open-loop and closed-loop postural control mechanisms, Exp. Brain Res. 104 (1995) 480–492.
[3] H. Corriveau, R. Hebert, F. Prince, M. Raiche, Intrasession reliability of the "center of pressure minus center of mass" variable of postural control in the healthy elderly, Arch. Phys. Med. Rehabil. 81 (2000) 45–48.
[4] H. Corriveau, R. Hebert, F. Prince, M. Raiche, Postural control in the elderly: an analysis of test–retest and interrater reliability of the COP–COM variable, Arch. Phys. Med. Rehabil. 82 (2001) 80–85.

[5] H. Corriveau, R. Hebert, M. Raiche, M.F. Dubois, F. Prince, Postural stability in the elderly: empirical confirmation of a theoretical model, Arch. Gerontol. Geriatr. 39 (2004) 163–177.
[6] H. Corriveau, R. Hebert, M. Raiche, F. Prince, Evaluation of postural stability in the elderly with stroke, Arch. Phys. Med. Rehabil. 85 (2004) 1095–1101.
[7] H. Corriveau, F. Prince, R. Hebert, M. Raiche, D. Tessier, P. Maheux, J.L. Ardilouze, Evaluation of postural stability in elderly with diabetic neuropathy, Diabetes Care 23 (2000) 1187–1191.
[8] P. Era, E. Heikkinen, Postural sway during standing and unexpected disturbance of balance in random samples of men of different ages, J. Gerontol. 40 (1985) 287–295.
[9] W.H. Gage, D.A. Winter, J.S. Frank, A.L. Adkin, Kinematic and kinetic validity of the inverted pendulum model in quiet standing, Gait Posture 19 (2004) 124–132.
[10] P. Gatev, S. Thomas, T. Kepple, M. Hallett, Feedforward ankle strategy of balance during quiet stance in adults, J. Physiol. 514 (Pt 3) (1999) 915–928.
[11] P.A. Goldie, T.M. Bach, O.M. Evans, Force platform measures for evaluating postural control: reliability and validity, Arch. Phys. Med. Rehabil. 70 (1989) 510–517.
[12] F.B. Horak, C.L. Shupert, A. Mirka, Components of postural dyscontrol in the elderly: a review, Neurobiol. Aging 10 (1989) 727–738.
[13] A. Karlsson, G. Frykberg, Correlations between force plate measures for assessment of balance, Clin. Biomech. (Bristol. Avon) 15 (2000) 365–369.
[14] A. Karlsson, H. Lanshammar, Analysis of postural sway strategies using an inverted pendulum model and force plate data, Gait Posture 5 (1997) 198–203.
[15] D.L. King, V.M. Zatsiorsky, Extracting gravity line displacement from stabilographic recording, Gait Posture 6 (1997) 27–38.
[16] D. Lafond, M. Duarte, F. Prince, Comparison of three methods to estimate the center of mass during balance assessment, J. Biomech. 37 (2004) 1421–1426.
[17] I.D. Loram, C.N. Maganaris, M. Lakie, Active, non-spring-like muscle movements in human postural sway: how might paradoxical changes in muscle length be produced? J. Physiol. 564 (2005) 281–293.
[18] I.D. Loram, C.N. Maganaris, M. Lakie, Human postural sway results from frequent, ballistic bias impulses by soleus and gastrocnemius, J. Physiol. 564 (2005) 295–311.
[19] B.E. Maki, P.J. Holliday, G.R. Fernie, Aging and postural control. A comparison of spontaneous- and induced-sway balance tests, J. Am. Geriatr. Soc. 38 (1990) 1–9.
[20] B.E. Maki, P.J. Holliday, A.K. Topper, A prospective study of postural balance and risk of falling in an ambulatory and independent elderly population, J. Gerontol. 49 (1994) M72–M84.
[21] B.E. Maki, W.E. McIlroy, Postural control in the older adult, Clin. Geriatr. Med. 12 (1996) 635–658.
[22] K. Masani, M.R. Popovic, K. Nakazawa, M. Kouzaki, D. Nozaki, Importance of body sway velocity information in controlling ankle extensor activities during quiet stance, J. Neurophysiol. 90 (2003) 3774–3782.
[23] C. Maurer, R.J. Peterka, A new interpretation of spontaneous sway measures based on a simple model of human postural control, J. Neurophysiol. 93 (2005) 189–200.
[24] P.G. Morasso, M. Schieppati, Can muscle stiffness alone stabilize upright standing? J. Neurophysiol. 82 (1999) 1622–1626.
[25] M.P. Murray, A.A. Seireg, S.B. Sepic, Normal postural stability and steadiness: quantitative assessment, J. Bone Joint Surg. Am. 57 (1975) 510–516.
[26] V.P. Panzer, S. Bandinelli, M. Hallett, Biomechanical assessment of quiet standing and changes associated with aging, Arch. Phys. Med. Rehabil. 76 (1995) 151–157.
[27] R.J. Peterka, Sensorimotor integration in human postural control, J. Neurophysiol. 88 (2002) 1097–1118.
[28] R.J. Peterka, Simplifying the complexities of maintaining balance, IEEE Eng. Med. Biol. Mag. 22 (2003) 63–68.
[29] T.E. Prieto, J.B. Myklebust, R.G. Hoffmann, E.G. Lovett, B.M. Myklebust, Measures of postural steadiness: differences between healthy young and elderly adults, IEEE Trans. Biomed. Eng. 43 (1996) 956–966.
[30] L. Rocchi, L. Chiari, A. Cappello, Feature selection of stabilometric parameters based on principal component analysis, Med. Biol. Eng. Comput. 42 (2004) 71–79.
[31] P. Rougier, O. Caron, Center of gravity motions and ankle joint stiffness control in upright undisturbed stance modeled through a fractional Brownian motion framework, J. Mot. Behav. 32 (2000) 405–413.
[32] P. Rougier, I. Farenc, Adaptative effects of loss of vision on upright undisturbed stance, Brain Res. 871 (2000) 165–174.
[33] D.A. Winter, Biomechanics and Motor Control of Human Movement, John Wiley & Sons Inc., Toronto, 1990.
[34] D.A. Winter, A.E. Patla, F. Prince, M. Ishac, K. Gielo-Perczak, Stiffness control of balance in quiet standing, J. Neurophysiol. 80 (1998) 1211–1221.
[35] V.M. Zatsiorsky, D.L. King, An algorithm for determining gravity line location from posturographic recordings, J. Biomech. 31 (1998) 161–164.

ELSEVIER

Journal of Biomechanics 40 (2007) 3114–3120

JOURNAL OF BIOMECHANICS

www.elsevier.com/locate/jbiomech
www.JBiomech.com

In vivo behavior of muscle fascicles and tendinous tissues in human tibialis anterior muscle during twitch contraction

Toshiaki Oda[a,*], Ryutaro Himeno[a], Dean C Hay[b], Kentaro Chino[c], Toshiyuki Kurihara[d], Toshihiko Nagayoshi[e], Hiroaki Kanehisa[d], Tetsuo Fukunaga[f], Yasuo Kawakami[f]

[a]*Computational Biomechanics Unit, RIKEN, Saitama, Japan*
[b]*Graduate School of Interdisciplinary Information Studies, University of Tokyo, Tokyo, Japan*
[c]*Japan Institute of Sports Sciences, Tokyo, Japan*
[d]*Department of Life Sciences, University of Tokyo, Tokyo, Japan*
[e]*Graduate School of Human Sciences, Waseda University, Saitama, Japan*
[f]*Faculty of Sports Sciences, Waseda University, Saitama, Japan*

Accepted 22 March 2007

Abstract

In this study we investigated the time course of length and velocity of muscle fascicles and tendinous tissues (TT) during isometric twitch contraction, and examined how their interaction relates to the time course of external torque and muscle fascicle force generation. From seven males, supra-maximal twitch contractions (singlet) of the tibialis anterior muscle were induced at 30°, 10° and −10° plantar flexed positions. The length and velocity of fascicles and TT were determined from a series of their transverse ultrasound images. The maximal external torque appeared when the shortening velocity of fascicles was zero. The fascicle and TT length, and external torque showed a 10–30 ms delay of each onset, with a significant difference in half relaxation times at −10°. The time course of TT elongation, and fascicle and tendinous velocities did not differ between joint angles. Curvilinear length–force properties, whose slope of quasi-linear part was ranged from −15.0 to −5.9 N/mm for fascicles and 5.4 to 14.3 N/mm for TT, and a loop-like pattern of velocity–force properties, in which the mean power was ranged from 0.14 to 0.80 W for fascicles, and 0.14 to 0.81 W for TT were also observed. These results were attributed to the muscle–tendon interaction, depending on the slack and non-linearity of length–force relationship of compliant TT. We conclude that the mechanical interaction between fascicles and TT, are significant determinants of twitch force and time characteristics.

Keywords: Muscle–tendon interaction; Twitch time characteristics; Compliant tendinous tissues; Muscle fibers; Ultrasound images

1. Introduction

In live human experiments, evoked twitch contraction has been studied for the parameters including peak force, time to peak force, and half relaxation time, to estimate physiological properties of muscles and their changes induced by experimental protocols (e.g. fatigue: Bigland-Ritchie et al., 1983; Shields et al., 1997; Lepers et al., 2002, training: McDonagh et al., 1983, and bed rest: Davies et al., 1987). Unlike experiments with the excised muscle fibers, however, in vivo muscle fibers connect in series to compliant tendinous tissues (tendon + aponeuroses; TT) that elongate under tension and become slack when the muscle tendon complex (MTC) is in a shortened, rested state. In human experiment, Loring and Hershenson (1992) showed that the peak twitch force was smaller when the muscle is allowed to shorten against external series compliance compared with an isometric condition. Also, the dependence of time to peak of twitch torque on the stiffness of TT (Pearson and Onambele, 2006), and a significant positive correlation between electromechanical delay and the amount of stretch from resting state in TT

*Corresponding author. Tel.: +81 48 462 1111x3892; fax: +81 48 467 9610.
E-mail address: toda@riken.jp (T. Oda).

0021-9290/$ - see front matter © 2007 Elsevier Ltd. All rights reserved.
doi:10.1016/j.jbiomech.2007.03.023

(Morse et al., 2005) have been demonstrated. These findings suggest that the compliant TT, by interacting with muscle fibers, has considerable influence on the parameters of twitch torque.

In addition, several previous studies have pointed out that the interaction between muscle fibers and TT has a considerable effect on the force development of the MTC during fixed end contractions (Kawakami and Lieber, 2000; Lieber et al., 1992; Hawkins and Bey, 1997). The muscle fibers' force during a contraction is a function of length and velocity of muscle fibers (van Zandwijk et al., 1996, 1998). Therefore, in order to relate the time course of twitch torque with physiological properties of muscle fibers, it is important to understand not only the time course of twitch torque, but also the length–velocity–force properties of muscle fibers resulting from the interaction with TT. However, information is limited on the behavior of human in vivo muscle fibers and TT during twitch contraction and their roles in developing external torque.

The measurements of length change in fascicles (bundles of muscle fibers) and TT can be achieved via B-mode ultrasonography (Herbert and Gandevia, 1995; Fukunaga et al., 1997) as well as TT (Ito et al., 2000; Kubo et al., 2002). In this study, we investigated the time course of length and velocity in both muscle fascicles and TT during isometric twitch contraction, and examined how their behavior relates to the time course of external torque and muscle fascicle force (FF) generation.

2. Methods

Seven healthy males (age, 24.0±2.3 years; height, 173.2±5.4 cm; weight, 67.8±4.3 kg; means±S.D.) participated voluntarily in the present study. The subjects were fully informed of the purpose and the procedures of this study, after which each gave their written consent to participate.

2.1. Experimental design

Each subject sat on the bench of a joint torque measurement machine (VTF-002R/L, VINE, Japan), with knees fully extended. The right foot was secured to an adjustable footplate by non-elastic strapping. To examine the effects of initial muscle fiber and MTC length on the force development parameters, plantar flexion angles of 30° and 10° (30° and 10°), and a dorsi-flexion angle of 10° (−10°) were used (anatomical position = 0°). Twitch contractions of the tibialis anterior (TA) muscle were induced by supra-maximal electrical stimulus; singlet to the common peroneal nerve. For each joint angle, eight twitches were induced. The first five twitches were used as conditioning stimuli, followed by three trial stimuli during which ankle torque, the soleus muscle (SOL) and TA electromyography, and ultrasonic images of TA were recorded with 2 min between each twitch. There was at least a 5 min interval between different joint angle trials.

2.2. Electrical stimuli

A 500 μs single supra-maximal electrical stimulus to the common peroneal nerve from a high-voltage stimulator and specially modified isolator (SEN-3301 & SS-1963, Nihon Koden, Japan) was used. The cathode electrode (1 cm diameter) was put over the head of the fibula and the anode electrode (5 cm × 7 cm square sheet) was placed over the tibial tuberosity (Thomas et al., 1989). To confirm that the stimulating position and intensity were correct, muscle compound action potentials (M wave) were recorded using surface electrodes (Blue sensor P-00-S, Ambu, Denmark). The recording electrodes with a diameter of 10 mm and an inter-electrode distance of 20 mm were put on the distal position of the mid-belly of TA and SOL of the right leg. The recorded M waves were A/D converted at a sampling rate of 2 kHz (MacLab/16SP, ADInstruments, Australia) and stored in a personal computer. Using sub-maximal stimuli, the position of the stimulating electrodes was adjusted until both twitch peak torque and M wave amplitude of TA were maximized and where SOL M wave activity was absent. Once the optimal position had been determined, the stimulus intensity was increased to the supra-maximal level, resulting in no further changes to the M wave amplitudes of the TA. For each change in ankle angle, these procedures were repeated.

2.3. Recording of TA ultrasonic images

A real-time B-mode ultrasonic apparatus (SSD-6500SV, Aloka, Japan) with an electronic linear-array probe (7.5 MHz wave frequency with 60 mm scanning length; UST 5047-5, Aloka, Japan) was used to obtain a longitudinal ultrasonic image of TA, 40% distally from the knee (measured from the popliteal crease to the center of the lateral malleolus). The probe position and imaging plane were carefully adjusted to obtain echo images in which the superficial and central aponeuroses were parallel to each other, and the plane is parallel to the fascicles; otherwise, the length of fascicles and TT, and pennation angle (PA) would be misestimated (Scott et al., 1993; Kawakami et al., 1998; Klimstra et al., 2006). The images during twitch contraction were recorded at 96.37 Hz to a computer memory of the ultrasonic apparatus (this frequency is dependent on the frame size of image), before they were sent to a personal computer as JPEG-formatted images for subsequent analyses. A square wave electrical pulse was used as a trigger to synchronize the collection of ultrasound images and other data (torque, electromyography, and stimulus signals) stored in the computer.

2.4. Data analysis

2.4.1. Fascicle length, pennation angle and elongation of tendinous tissues

The muscle fascicle length (FL), PA and TT elongation (TTE) were measured using ImageJ 1.36b (National Institutes of Health, USA). A trial clearly showing cross points at which fascicles attached to the superficial and deep aponeuroses was selected for analysis. The cross points between a fascicle and aponeuroses were digitized from the serial ultrasonic images during twitch contraction. In cases where the cross points between the fascicle and aponeuroses exceeded the boundaries of the ultrasound image, linear extrapolation was used. The method of linear extrapolation in the present study was similar to the method used by Maganaris and Baltzopoulos (1999). Digitizing was performed three times and the mean value was then used for descriptive data analyses. FL was calculated as the straight line distance between the digitized points of proximal and distal ends of the fascicle, while PA was defined as the angle between the fascicle and deep aponeurosis. The minimal FL (FL_{min}), time to minimal FL ($FL_{min\text{-}time}$), and FL half relaxation time (FL_{HRT}) were determined. $FL_{min\text{-}time}$ was defined as the time from stimulus to FL_{min}. FL_{HRT} was defined as the duration for the fascicle to return from FL_{min} to half the length of initial FL. TTE was measured using the method described by Kubo et al. (2002). Briefly, the elongation was determined from the movement of cross points between a fascicle and aponeurosis connecting to the distal tendon. The maximal TTE (TTE_{max}), time to maximal TTE ($TTE_{max\text{-}time}$), and TTE half relaxation time (TTE_{HRT}) were determined in the same way as the fascicle parameters. Additionally, velocities for the fascicles and TT (FV and TTV) were calculated by differentiating the time course of length changes.

The ensemble coefficients of variation of the measurements (data from the number of images × 7 subjects × 3 angles × 3 analyses) were 0.7±1.1% for the absolute FL and 18.7±67.1% for the absolute TTE. The larger coefficient of variation for the latter was due to the very small absolute

value of TTE (maximal 5.3 mm). The ensemble inter-class correlation of three analyses was more than 0.99 for both FL and TTE. The time resolution (10.37 ms between images) of the parameters with the ultrasound method have been discussed elsewhere (Oda et al., 2006). Twitch parameters are thus limited to this time resolution. However, the Nqvist frequency was 48.19 Hz, which we judged would be enough to measure length changes during a twitch contraction.

2.4.2. External torque, tendon and fascicle forces

Firstly, the maximal external torque (ET_{max}), time to maximal external torque ($ET_{max\text{-}time}$) and external torque half relaxation time (ET_{HRT}) were calculated in the same manner as described in Section 2.4.1. Secondly, tendon force (TF) and FF were determined from the external dorsi-flexion torque (ET). The TF transmitted through TT was calculated using the following equation:

$$TF = k\frac{ET}{MA},$$

where k is the relative physiological cross-sectional area contribution (0.57) of the TA to all dorsi-flexor muscles (Wickiewicz et al., 1983), ET is the external measured torque, and MA is the length of the TA moment arm at each joint angle (Rugg et al., 1990). The FF was calculated by dividing the TF by the cosine of the PA (Kawakami et al., 2000).

2.5. Statistics

A two-way repeated ANOVA (parameter × joint angle) was used to test differences in each time to peak and half relaxation time between related parameters (e.g. $FL_{min\text{-}time}$ vs. $TTE_{max\text{-}time}$ vs. $ET_{max\text{-}time}$). As for other parameters, a one-way repeated ANOVA was used for comparisons between the three joint angles. Tukey's HSD analysis was selected for multiple comparisons. The level of significance for all statistical analyses was set at $p<0.05$.

3. Results

3.1. Time course data

The group ensemble averages of time course data are displayed in Fig. 1. The fascicles initially shortened and then lengthened. TT exhibited an opposite pattern of elongation followed by shortening. There was a delay of 10–30 ms between the onset of length changes in both fascicles and TT, and the development of ET. ET_{max} was observed when the shortening velocity of fascicles was zero. The maximal FV appeared in the initial phase (average: 33 ± 16 ms) of contraction. Despite angle-dependent changes in FF and TF, the time course of TTE, FV and TTV did not vary significantly over different angles. These tendencies were commonly observed in all subjects.

3.2. Descriptive data

Fig. 2 shows the results of the time to peak and the half relaxation time. Each $FL_{min\text{-}time}$, $TTE_{max\text{-}time}$ and $ET_{max\text{-}time}$ had no significant difference between joint angles. In comparison between parameters, FL_{HRT} and TTE_{HRT} were both significantly longer than ET_{HRT} in the −10° condition. ET_{HRT} was significantly greater at 30° compared with −10°, and non-significantly greater than 10°.

The other descriptive data for the parameters of fascicles and TT are summarized in Table 1. Resting FL and FL_{min} significantly differed between all joint angles, while

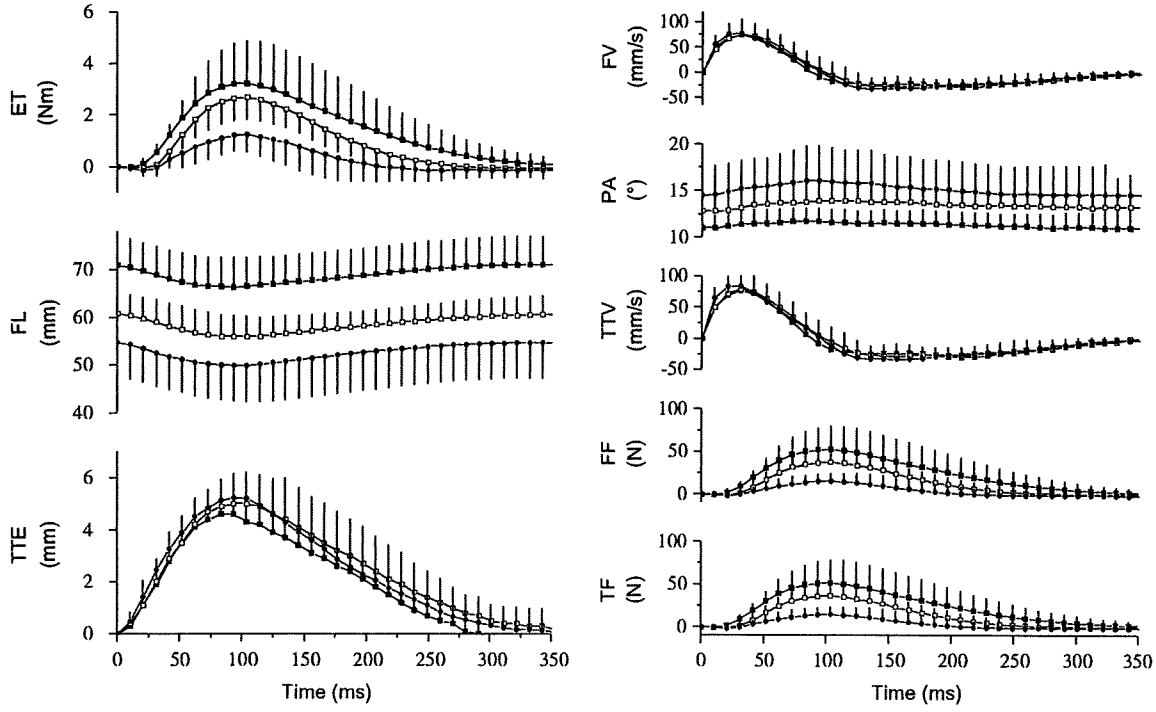

Fig. 1. Group ensemble averages ± standard deviation ($n = 7$) of the time-course of change in external torque (ET), fascicle length (FL), elongation of tendinous tissues (TTE), fascicle velocity (FV), pennation angle (PA), lengthening velocity of tendinous tissues (TTV), fascicle force (FF) and tendon force (TF) [(■) 30°, (□) 10°, and (●) −10°]. Zero on the horizontal axis indicates the moment at which the electrical stimulus was delivered.